



저작자표시-비영리-변경금지 2.0 대한민국

이용자는 아래의 조건을 따르는 경우에 한하여 자유롭게

- 이 저작물을 복제, 배포, 전송, 전시, 공연 및 방송할 수 있습니다.

다음과 같은 조건을 따라야 합니다:



저작자표시. 귀하는 원저작자를 표시하여야 합니다.



비영리. 귀하는 이 저작물을 영리 목적으로 이용할 수 없습니다.



변경금지. 귀하는 이 저작물을 개작, 변형 또는 가공할 수 없습니다.

- 귀하는, 이 저작물의 재이용이나 배포의 경우, 이 저작물에 적용된 이용허락조건을 명확하게 나타내어야 합니다.
- 저작권자로부터 별도의 허가를 받으면 이러한 조건들은 적용되지 않습니다.

저작권법에 따른 이용자의 권리는 위의 내용에 의하여 영향을 받지 않습니다.

이것은 [이용허락규약\(Legal Code\)](#)을 이해하기 쉽게 요약한 것입니다.

[Disclaimer](#)

A THESIS
FOR THE DEGREE OF MASTER OF ENGINEERING

**Development of Hybrid Generator using
Triboelectric-Electromagnetic Components for
Scavenging Wind and Water Wave Energy**

WOO JOONG KIM

Department of Mechatronics Engineering
GRADUATE SCHOOL
JEJU NATIONAL UNIVERSITY

February 2020

Development of Hybrid Generator using Triboelectric-Electromagnetic Components for Scavenging Wind and Water Wave Energy

WOO JOONG KIM

(Supervised by Professor Sang Jae Kim)

A thesis submitted in partial fulfillment of the requirement for the degree of
Master of Engineering

2019.12

The thesis has been examined and approved.

Thesis Director Professor, Department of Mechatronics Engineering,
Prof. Joung-Hwan Lim College of Engineering, Jeju National University

Thesis Committee Member Professor, Department of Mechatronics Engineering,
Prof. Chul-ung Kang College of Engineering, Jeju National University

Thesis Committee Member Professor, Department of Mechatronics Engineering,
Prof. Sang-Jae Kim College of Engineering, Jeju National University

December, 2019

**Department of Mechatronics Engineering
GRADUATE SCHOOL
JEJU NATIONAL UNIVERSITY**

Acknowledgements

I would like to express my sincere gratitude to all who have supported, contributed to the completion of this master thesis. I experienced and crossed the hard paths, failures and many achievements during this research work. I am so grateful to the people who guidance, help and encouragement.

First and foremost, I would like to express my sincere and deep gratitude to my research advisor, **Prof. Sang-Jae Kim**, Jeju National University, for supervision and giving me the opportunity to execute the research work. I thank him for his support, encouragement and suggestion on the research work through personal discussions and periodical lab meetings.

I express my thanks to my former lab member and my mentor, **Dr. Arunkumar Chandrasekhar**, for his kind guidance in experiment and his help in learning the basics of energy harvesting. I extend my thanks express thanks to mentor, **Mr. Venkateswaran Vivekananthan**, for his help and guidance during the entire research work. I also extend my thanks to my mentor, **Mr. Gaurav Khandelwal**, for his help and support during my research work. I would also thank all the members of nanomaterials and systems laboratory **Dr. Karthi, Dr. Alluri, Dr. Yuvasree, Dr. Natarajan, Dr. Dipak, Mr. Surjit, Mr. Nirmal, Ms. Sindhuja, Mr. Abishek, Mr. Dhanasekar, Mr. Swapnil, Mr. Sugato, Mr. Arun, Ms. Manisha and Ms. Aparna.**

I express my thanks to **Prof. Joung-Hwan Lim** and **Prof. Chul-ung Kang** for their kind support during my course work studies and their encouragement during the research. Also, I thank them for being the thesis review committee members and providing valuable suggestions on improving the quality of my thesis. I

would thank **Mr. Cho Inho**, **Ms. Lee Hyun Seok**, and **Mr. Kim Chan** for their help in official works and documents processing.

Last but certainly not least, my earnest gratitude to my parents **Mr. Kim Young Hak** and **Mrs. Hong Young Ja** for their encouragement and support for my studies and providing me all the required facilities and wishing me all my dreams to come true. My thanks are unbounded for their unconditional love, support and care.

Kim Woo Joong

CONTENTS

Contents	i
Nomenclature	iii
List of figures	iv
List of tables	viii
초 록	ix
Abstract	xi
1. Introduction	
1.1 Introduction	1
1.2 Working modes of TENG	3
1.2.1 Contact separation mode	5
1.2.2 Linear Sliding mode	5
1.2.3 Single electrode mode	5
1.2.4 Free-standing mode	6
2. Materials and methods	
2.1 Materials used	8
2.2 Materials Characterization and Measurements	9
2.2.1 Field emission scanning electron microscope (FE-SEM)	9
2.2.2 Sputter coating	9
2.2.3 Reactive ion etching	9
2.2.4 Linear Motor	10
2.2.5 Electrometer	10
3. Development of tubular shape triboelectric-electromagnetic hybrid generator for blue energy scavenging and oil spill detection	
3.1 Experimental Section	12
3.1.1 Device fabrication and measurements	12
3.2 Working mechanism	13
3.3 Results and discussions	15

3.4 Conclusion	25
4. Development of Wind Energy harvesting hybrid generator made of Triboelectric and Electromagnetic components for wind speed and Wind direction monitoring	
4.1 Experimental Section	27
4.1.1 Device fabrication and measurements	27
4.2 Results and discussions	28
4.3 Conclusion	34
5. References	35
Appendix: Publications	41
Appendix: Conferences	42
Appendix: List of awards	44
Declaration	45

Nomenclature

TENG	Triboelectric nanogenerator
EMG	Electromagnetic generator
PMU	Power Management Unit
DI	Deionized Water
LED	Light Emitting Diode
FE-SEM	Field Emission Scanning Electron Microscope
PET	Polyethylene terephthalate
SCCM	Standard cubic centimeter per minute
MEMS	Micro-electromechanical Systems
NEMS	Nano-electromechanical Systems
PVD	Pulsed vapor deposition

List of Figures

Figure 1.1.1	Triboelectric series chart showing materials with their charges	2
Figure 1.2.1	Schematic representation of the four fundamental operating modes of TENG	4
Figure 3.1.1	Schematic diagram of the TENG component with different layers present in the device and the inset shows an FE-SEM image showing the surface roughness made using the Kapton film. The right hand side image shows the EMG components with coils attached and its layers	13
Figure 3.2.1	Working mechanism of TENG and EMG components of the blue energy harvesting hybrid device. The TENG component works on linear sliding mode with the magnet slides over the Kapton film generating electrical output and with the similar motion the magnet moves over the coil wound on the outer side of the PET tube leading to the generation of electric flux in EMG component	14
Figure 3.3.1	(a) and (b) voltage and current output of TENG component (c) and (d) voltage and current output of EMG component	16
Figure 3.3.2	(a) and (b) voltage and current response of EMG output with both coils connected in series connection for voltage and parallel connection for current measurements	17
Figure 3.3.3	(a) and (b) voltage and current response of TENG, EMG, TENG + 1 EMG and TENG + 2 EMG compositions (c) stability test of TENG for a period of 2000s using linear motor	18
Figure 3.3.4	(a) and (b) force analysis of TENG component (c) and (d) force analysis of EMG component	19
Figure 3.3.5	(a) circuit diagram of capacitor charging and LED lit up (b) high power white, green and red LED lit put using the	20

	bridge rectifier circuit and a set of 80 low power green LEDs glowing using hybrid connections	
Figure 3.3.6	(a) powering up a commercial calculator using the hybrid device with charging a commercial capacitor (b) powering up of a commercial humidifier for a period of 30 seconds by charging a commercial capacitor	21
Figure 3.3.7	Power management circuit for the real-time application and (b) shows the real-time image of the developed power management unit and the demonstration of lighting up an white LED using the circuit	21
Figure 3.3.8	(a) schematic of the oil spill detection system using the hybrid generator with and without oil (b) two distinct layers of oil and water showing that the oil spill will be on the top of the water due to the high viscosity (c) real time demonstration of oil-spill detection in lab conditions (d) (i-vii) oil spill detection with respect to change in conductivity of the solution with the LED glowing. The trial was made by selecting water samples such as 1 M NaCl solution, sea water, tap water, DI water, oil, oil in sea water and oil in NaCl	22
Figure 3.3.9	Schematic of wireless oil spill identification using Bluetooth interface with mobile phone	23
Figure 3.3.10	(a) blue energy device made with buoy shape which can float in water had setup with the Arduino board and Bluetooth device. (b) and (c) the change in conductivity will be informed by Bluetooth messaging and an LED lit up in the buoy	23
Figure 4.1.1	Schematic of Flutter based hybrid device for scavenging wind energy with TENG and EMG components working simultaneously	27
Figure 4.1.2	Various active layers of the wind energy harvesting hybrid generator device with EMG coil, Kapton Layer and	28

Aluminum layer. The friction between Aluminum and Kapton works as TENG component and the EMG coil with magnet generates the EMG component

- Figure 4.2.1 (a-d) surface morphology of the Kapton film made with the plasma etching process. The surface shows various roughness according to the etching conditions (e) voltage response of Kapton film made with different surface roughness 29
- Figure 4.2.2 Electrical output response of the TENG component (a and b) voltage and current output response of the TENG component (c and d) voltage and current of TENG component under different acceleration (e) lead resistance analysis of TENG component with its instantaneous peak power of 225 μW under the resistance of 100 $\text{M}\Omega$ and (f) stability test of TENG for a period of 1000 s at 12 m/s^2 acceleration 31
- Figure 4.2.3 Electrical output response of the EMG component (a and b) voltage and current output response of the TENG component (c and d) voltage and current of EMG component under different acceleration (e) lead resistance analysis of EMG component with its instantaneous peak power of 0.8 mW under the resistance of 100 Ω and (f) stability test of EMG for a period of 1000 s at 12 m/s^2 acceleration 31
- Figure 4.2.4 (a) circuit diagram for charging capacitor and LED lit up connected with TENG and EMG components (b) Capacitor charging using TENG, EMG and Hybrid connections (c) glowing 100 green LEDs using hybrid combination of the flutter based device 32

Figure 4.2.5 (a to d) real-time output analysis of the flutter based hybrid 33
device with 4 devices positioned at various directions to
monitor the wind direction (e) real-time speed monitoring
under low and high speed in comparison with (f) which is
measured using linear motor under different accelerations

List of Table

Table 2.1	Table showing materials and methods used for this research	8
Table 3.3.1	Conductivity of various water samples	24
Table 4.1	Showing the conditions with respect to gas level (in sccm)	29

초 록

화석 연료 사용으로 인한 지구 온난화 및 오염과 같은 환경 문제가 증가하기 때문에 저전력 소비자 전자 기기에 전원을 공급하기 위한 지속 가능한 전원을 개발하는 것이 매우 중요하다. 또한 지금까지 사용된 화석 연료가 다시 생성될 때까지 수천 년이 걸릴 것이다. 이러한 환경 문제를 극복하기 위해 연구원들은 지속 가능하며 깨끗한 에너지를 개발해 왔다. 나노발전기의 발명은 일상생활에서 버려지는 기계적 에너지를 통해 녹색 에너지를 생산할 수 있는 길을 열어준다. TENG (Triboelectric Nanogenerator) 및 PENG (Piezoelectric Nanogenerator)과 같은 나노발전기는 외부의 기계적 힘이 가해질 때 각각 마찰 전기 효과 및 압전 효과에 의해 발전한다. 사람의 보행, 파도, 진동 등으로부터 기계 에너지를 쉽게 찾을 수가 있으며 이것은 유용한 전기 에너지로 쉽게 변환 할 수 있다. TENG 및 PENG에서 개별적으로 생성된 전력은 다양한 전자 장치에 전력을 공급하기에 충분할 정도로 효율적이지 않다. 이러한 발전기의 전력 및 전력 밀도는 다양한 실시간 어플리케이션을 수행하기에는 부족하다. 이 문제를 극복하기 위해, 다른 나노발전기를 단일 유닛으로 조합함으로써 하이브리드 나노발전기를 제작하였다.

최근에는 TENG-PENG, NGs-Solar cell, NGs-electromagnetic generator (EMG)와 같은 하이브리드 나노발전기가 여러 논문에 소개되었으며, 각각의 발전기는 고유의 장점 및 단점들이 있다. 본 학위 논문에서는 파도와 바람으로부터 기계적 에너지를 전기 에너지로 바꾸기 위하여 TENG과 EMG로 이루어진 하이브리드 발전기가 다양한 형태의 단일 유닛형태로 제작되었다. 한 장치는 코일이 두 군데 감긴 튜브형 구조로 제작되었다. 튜브의 안쪽 면은 전극이 코팅된 캡톤 필름이 배치되었다. 튜브의 내부에는 네오디뮴자석이 있으며, 이 자석이 튜브 내부에서 미끄러지며 마찰 전위를 발생시킴과 동시에 코일

내부를 이동하며 EMG 전위를 발생시키는 과정을 통하여 자석의 기계적 에너지를 전기 에너지로 변환하게 된다. 이 튜브형 발전기는 부표 내부에 위치하는 것을 고려하여 제작되었으며, 그 부표는 수면 위에 떠 있는 상태에서 파도에 의한 기계적 에너지를 전기 에너지로 변환하게 된다.

다른 형태의 하이브리드 발전기는 풍력 발전을 위하여 필러이는 형태의 TENG-EMG로 이루어져 있다. 가벼운 캡톤 필름의 한 면은 접점을 향상시켜 높은 마찰출력을 얻기 위해 플라즈마 에칭 공정을 통하여 표면 거칠기를 형성시켰으며 다른 한 면은 전극이 코팅되었다. 또한 면 형태의 경량 구리 코일이 부착되었으며, 이 캡톤 필름은 알루미늄과 더불어 아크릴로 만들어진 터널 내부에 배치되었다. 또한 네오디뮴자석도 배치되어 바람에 의해 캡톤 필름이 진동 형태의 운동을 하여 전기 출력을 효과적으로 생성 할 수 있다. 이러한 하이브리드 나노발전기들은 개별적인 나노발전기보다 효과적으로 높은 전기출력을 발생할 수 있으며 향후 밀리วัต (mW) 범위의 전력을 필요로 하는 IoT 분야에도 적용이 가능할 수 있다.

Abstract

Developing a sustainable power source for powering low power consumer electronic devices is very important because of increasing environmental issues such as global warming and pollution due to use of fossil fuels. Also, it will take thousands of years to recover the fossil fuels that have been utilized so far. To overcome these environmental issues, researchers have been developing a sustainable and clean energy source. The invention of nanogenerator paves the way for the generation of green energy through the waste mechanical energy in our day-to-day life. The nanogenerators such as triboelectric nanogenerator (TENG) and piezoelectric nanogenerators (PENGs) work on triboelectric effect and piezoelectric effect, respectively, upon actuating by an external mechanical force. Mechanical energy is abundant in the environment, such as human walking, water wave, vibrations, and can easily be utilized to convert into useful electrical energy. The generated electrical output from the TENGs and PENGs individually is not that efficient to power various electronic devices. The power and power density of these generators are not high to perform various real-time applications. In order to overcome this problem, hybrid nanogenerators were introduced by combining different energy harvesters in a single unit.

The hybrid nanogenerators such as TENG-PENG, NGs-Solar cell, NGs-electromagnetic generator (EMG) have been introduced in the recent past. Each component has its unique advantages and several drawbacks. Herein, a hybrid generator made of TENG and EMG in a single package with varying structures for scavenging mechanical energy from water wave and the wind has been fabricated. The device consists of a tubular-shaped structure with coils

wound on either side of the tubes. The inner portion of the tube has a kapton film with interdigitated electrode pattern, which acts as a triboelectric layer. The magnet is placed inside the tube, which slides over the kapton layer leads to the generation of triboelectric potential, and also the sliding magnet moves into the inner side of the coil developing the EMG potential upon simultaneous mechanical motions. The tubular structure is then placed into a buoy made of plastic and kept into the sea for scavenging the water wave motions. The buoy is then used for a real-time application of water spill detection.

The other type of hybrid generator made of TENG-EMG components for scavenging wind energy based on a flutter mechanism. A lightweight kapton film is used as a triboelectric layer with the creation of micro surface roughness using an inductively coupled plasma etching process. The roughness enhances the contact points leading to the generation of high triboelectric output. The other side of kapton film is coated with platinum for electrical connections. Also the kapton film is attached with a lightweight coil in a flat manner with a turn of 100 numbers. The kapton film is then placed inside an acrylic chamber with the inner top side attached with aluminum, which acts as a positive triboelectric layer as well as electrode. And the outer portion of acrylic on the top was attached with magnets for the generation of electromagnetic flux in the coil. These devices can effectively generate electrical output upon wind force and can also be used as wind speed and wind direction monitoring sensors. Thus the hybrid nanogenerators can scavenge electrical output effectively, which is much higher than the individual components and can also be used for many applications that require power in the range of milliwatts and can be used in the future internet of things (IoT).

CHAPTER 1

1.1 Introduction

Vibration is abundant and a vast amount is produced in the environment all over the time either naturally or by human-made. The generated vibrations are in the form of human motions, ocean waves, vehicle motions, wind, and heavy industries. The vibration energy harvesting in the past decades were done by using many conventional methods, requires high investment, capital cost and heavy machineries to convert wind into electricity. After the invention of nanogenerators, it has been reported that the wind energy can be scavenged easily in a cost-effective way. The intention of nanogenerators is to scavenge the waste mechanical energy and been used for powering up low power or small scale electronic devices. Also, the devices can also be used as a self-powered system for applications such as portable and wearable systems. Nanogenerators such as piezoelectric nanogenerator (PENG), triboelectric nanogenerator (TENG), and electromagnetic generator (EMG) are the devices used for vibration energy scavenging. Among these nanogenerator devices, TENG has shown enormous advantages such as simple fabrication, low cost, and lightweight. Other than harvesting vibration energy TENGs can be used to harvest most of the forms of mechanical energy such as wind, ocean, rotational, tidal and acoustic. However, TENG itself cannot produce high current to use for various real-time applications. So, a hybrid system is highly desirable to improve the efficiency of the TENG device, with the combination of two different energy harvesting modes in a single package. This type of hybrid generators can be used for boosting the electrical output performance of the nanogenerator and can also be able to improve the efficiency of the energy harvester. The hybrid energy harvesters, composed of TENG and EMG components had gained huge attention

because of its energy harvesting efficiency and performance under the simultaneous mechanical motions. TENG and EMG can work efficiently as a hybrid generator under sliding, contact-separation and rotation modes.

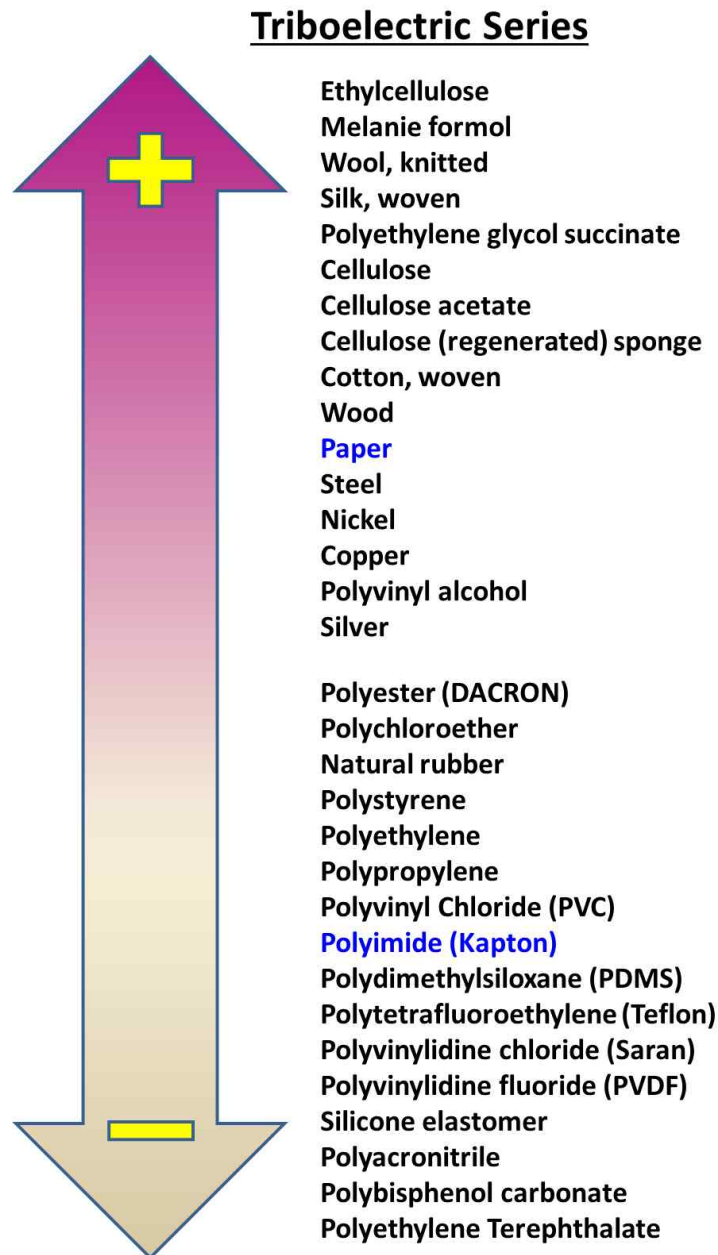


Figure 1.1.1 Triboelectric series chart showing materials with their charges

In the recent past a wide research is going on in the field of hybrid generator for scavenging mechanical energy and vibrational energy and eventually been used for various self-powered applications. A report by J. He et al. shows a TENG, PENG, and EMG components in a single unit for self-powered wireless monitoring system. Similarly, a report by H. Shao et al. shows the fabrication of a hybrid generator device with TENG and EMG components for scavenging water wave energy and this device has been used to operate an electronic thermometer. In both the above cases, the device uses a high cost and rugged construction, and also the device uses expensive triboelectric materials such as copper, carbon nanotubes, polyethylene terephthalate (PET). However, the device used in the present manuscript is used as the triboelectric material which is very cheap and simple in overall construction of the device. Since the device is a cylindrical type with the multi-unit energy harvesters and can harvest energy upon vibrational motions with various mechanical motions. The triboelectric components work on sliding mode triboelectrification made up of magnet and kapton as triboelectric material. Similarly the thesis work involves with different triboelectric materials based on their surface charges as shown in Figure 1.1.1. The material could not create damage on the Kapton layer due to friction like the traditional sliding mode triboelectric nanogenerator.

1.2 Working modes of TENG

The mechanism behind TENG is triboelectrification and electrostatic induction effects; with the rapid advancement in the field of nanogenerators and TENG, the exploration leads to the investigation of fundamental working modes of TENG which covers four basic modes. This includes a vertical contact separation mode, linear sliding mode, single electrode mode, and free-standing mode. These

modes require two different triboelectric materials with proper electrode connections with proper insulation between each layer. The combination may be either dielectric-dielectric or metal-dielectric arrangements. The basic principle behind all the four modes is that whenever there is a displacement in any of the triboelectric layers, the electrostatic charge movements break the electrostatic status present, leading to the development of potential difference between the electrodes. In the repeated mechanical actuation of layers with forward and reverse direction makes the triboelectric layer to generate forward and reverse potential between the electrodes. This makes the positive and negative peak in the TENG output generating the AC signal. The four different working modes are shown schematically in Figure 1.2.1.

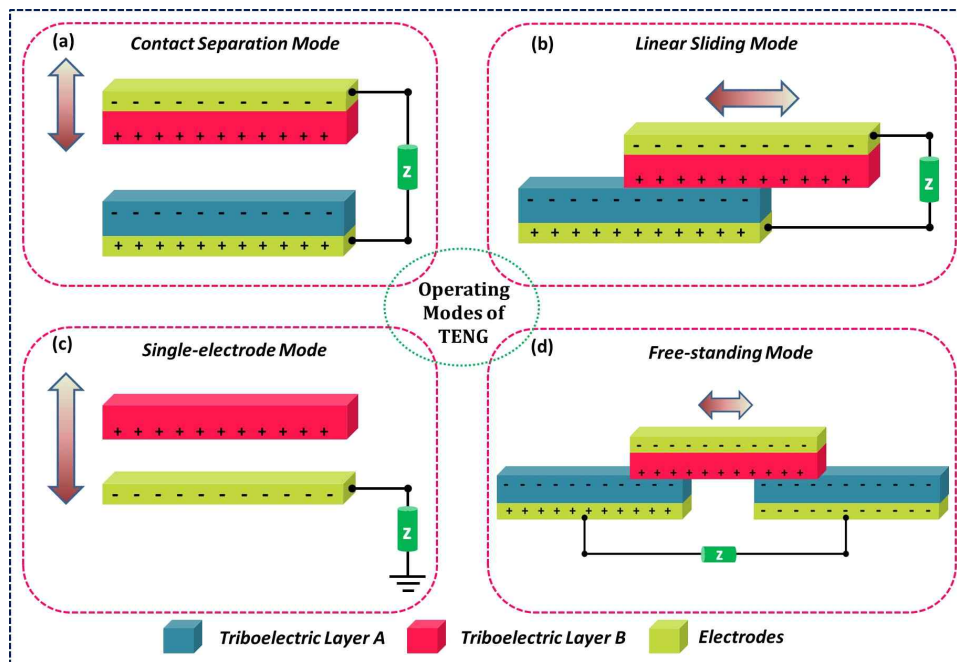


Figure 1.2.1 Schematic representation of the four fundamental operating modes of TENG

1.2.1 Contact separation mode

In the contact separation mode TENG, the triboelectrification occurs by the contact and separation process of two triboelectric materials or layers. This may either happen between two different dielectric materials or maybe a dielectric and metallic layers. This model has a high advantage with its simple design, easy fabrication, and low cost. This mode of TENG is also the first developed and demonstrated for powering low power electronics. This mode of TENG can be designed with a multi-unit stacking for the enhanced output performance. The simple contact separation mechanism is shown in Figure 1.2.1a.

1.2.2 Linear sliding mode

In the linear sliding mode, the charge generation is by the relative to and fro sliding between the layers of TENG. The construction is almost similar to the contact separation mode with electrodes attached on the back of the triboelectric layers, but the displacement is in sideward as shown in Figure 1.2.1b. The sliding mode has a low figure of merits compared to the vertical contact separation mode due to its long displacement in the sliding process. The advantage of this mode is that it can generate more charge density with a highly effective charge generation due to its high contact area. Also, by introducing more grating structures the output performance can be enhanced. The sliding mode TENG can also be able to operate in a rotational way with cylindrical grating structures.

1.2.3 Single electrode mode

The simplest structure of TENG is the single electrode mode TENG, but the output performance is too low due to the small charge transfer. This makes the generated voltage and current to be less, but it is highly suitable for

self-powered applications. The advantage of this device is, it overcomes the application limitation due to the contact wire obstructing at both sides in the contact separation mode and sliding mode TENG devices. The basic arrangement of a single electrode mode TENG is shown in Figure 1.2.1c.

1.2.4 Free-standing mode

The freestanding model has one electrode move freely between the two electrodes or triboelectric layers. The electrodes will be in a static position, and a triboelectric layer without electrode can move over it. This mode of TENG device has high figure of merits and has demonstrated high output efficiency and electrical output. Also, this type of device can be easily fabricated and can be integrated into various real-time applications. The basic arrangement of a single electrode mode TENG is shown in Figure 1.2.1d.

The present work describes the TENG-EMG hybrid generator which works simultaneously upon the same sliding motions. The device structure is aimed to employ both energy harvesters such as TENG and EMG. To fabricate a hybrid device composed of TENG and EMG components, the operating mode of the energy harvesting components needs to be considered. As we discussed that TENG has four working modes and the EMG, TENG components uses similar operating modes for scavenging waste mechanical energy. The device is fabricated for scavenging ocean wave energy, for that the suitable working mode is sliding mode TENG component. In consideration with the following merits and advantages we have chosen to fabricate a tubular shaped device comprising of TENG and EMG components with the TENG components operates on sliding mode with magnet slides over the Kapton film and the EMG component activates with the magnet moves inside the coils. To boost the current of the hybrid device the EMG component was made in both the sides of the tube. The

TENG component acts as a voltage source and the EMG component acts as a current source. The hybrid device combining both TENG and EMG with proper load matching resistance and rectification circuit the output power had been boosted and eventually been used for real-time demonstration such as charging the commercial capacitor and lighting up light-emitting diodes (LEDs). Further, the hybrid device had been used for scavenging small-scale biomechanical energy and also used for real-time oil spill detection. The flutter device can harvest electrical energy from the wind motion and also can work as wind direction monitoring and wind speed sensing. The enhanced output power generator with high efficiency would open door towards the field of MEMS/NEMS based applications in the near future with self-powered capability.

CHAPTER 2

Materials and Methods

2. 1 Materials Used

All materials used for this research are research grade and directly used without any further alterations. The list of materials including chemicals is given in the table below.

S. No	Materials	Supplier
1	Aluminum Foil	Dai Han, Korea
2	Aluminum Tape	Tae Kyung, Korea
3	Copper coil	Trox, korea
4	Copper wire	Trox, korea
5	Kapton film	DUPONT
6	Kapton tape	DUPONT
7	Polyethylene terephthalate (PET)	Hyosung chemicals
8	Neodymium magnets	Duratool
9	Sodium chloride (NaCl) (99 %)	Daejung Chemicals
10	Gold electrode (sputtered)	ACI alloys

Table 2.1 Table showing materials and methods used for this research

2.2 Materials Characterization and Measurements

2.2.1 Field emission scanning electron microscope (FE-SEM)

Field-emission scanning electron microscopy is a measurement tool used in the field of materials science for investigating the morphology of the material. The FE-SEM with EDAX can track the elements present in the material. The FE-SEM measurements carried out during this research was using TESCAN MIRA3.

2.2.2 Sputter coating

This deposition technique is a physical vapor deposition (PVD) technique. By using this technique targets of metallic and oxide based materials can be deposited on other substrate with the application of electric current on the material. The process requires a high vacuum inside the chamber to eject the material from the target placed inside the chamber. The sputtering process in general can be used for coating electrodes for the fabricated device layers. The sputtering measurements carried out during this research were using QUORUM Q150 RS.

2.2.3 Reactive ion etching

Reactive-ion etching (RIE) is an etching technology used in micro-fabrication. This is a type of dry etching which has different characteristics than wet etching. RIE uses chemically reactive plasma to remove material deposited on wafers. The plasma is generated under low pressure (vacuum) by an electromagnetic field. High-energy ions from the plasma attack the wafer surface and react with it. The RIE s carried out during this research were using RIE machine VITA.

2.2.4 Linear Motor

The linear motor is used for the continuous application of force on the device. The motor creates a periodical and continuous mechanical actuation with respect to time. The motor is controlled with a computer software which controls the operation of the motor. The electrical measurements in this research are carried out using a linear motor LinMot, InC, United States.

2.2.5 Electrometer

An electrometer is an instrument for the analysis or measurement of electric charge or potential difference in an electrical system. There are different types of electrometer systems, ranging from handmade mechanical instruments to high-precision electronic devices with different measurement ranges and impedance ranges. The measuring instrument used for the measurement of electrical output such as voltage and current is electrometer Keithley 6514 having a measurement range of peak to peak 400 V and 40 mA respectively. Also, for the measurement of current a low noise current amplifier SR 570 (Stanford instruments ltd.).

CHAPTER-3

Development of tubular shape triboelectric-electromagnetic hybrid generator for blue energy scavenging and oil spill detection

Highlights

- In the present a tubular shaped hybrid device composed of both EMG-TENG components for scavenging waste mechanical energy
- The tube is made of PET sheet rolled into a 20 mm cylinder and wound with copper coils for EMG and a kapton with gold electrode placed inside as TENG
- The magnet slides inside the tube creating the friction with Kapton to generate TENG output and the magnet moves inside the coils activates the EMG component
- The device generates an electrical output of 25 V /100 nA with TENG and 3 V/12 mA with EMG component
- The device has a capability of lighting up 80 green LEDs and charging a commercial capacitor using PMU
- Finally the device has been used for the real-time application of oil spill detection with the help of change in conductivity of the water

3.1 Experimental Section

3.1.1 Device fabrication and measurements

The device structure is aimed to employ both energy harvesters such as TENG and EMG. To fabricate a hybrid device composed of TENG and EMG components, the operating mode of the energy harvesting components needs to be considered. As we discussed that TENG has four working modes and the EMG, TENG components uses similar operating modes for scavenging waste mechanical energy. The device is fabricated for scavenging ocean wave energy, for that the suitable working mode is sliding mode TENG component. In consideration with the following merits and advantages we have chosen to fabricate a tubular shaped device made of PET had been used as the outer layer for the hybrid device (length is 120 mm and diameter is 20 mm) comprising of TENG and EMG components. A Kapton film was cut according to the size of the PET and coated with aluminum (Al) at the backside as the electrode material. The Kapton layer was kept as the inner wall and also acts as the negative triboelectric layer. Copper coils were wound on either side of the tube as shown in Figure 3.1.1 with 1500 turns has been wounded outside the cylinder for the EMG component. Further neodymium magnet (1/2" diameter and 1/4" thick) had placed inside the cylinder, where the sliding of magnet over the Kapton layer generates triboelectric potential and magnet moving into the coil activates the generation of electromagnetic induction.

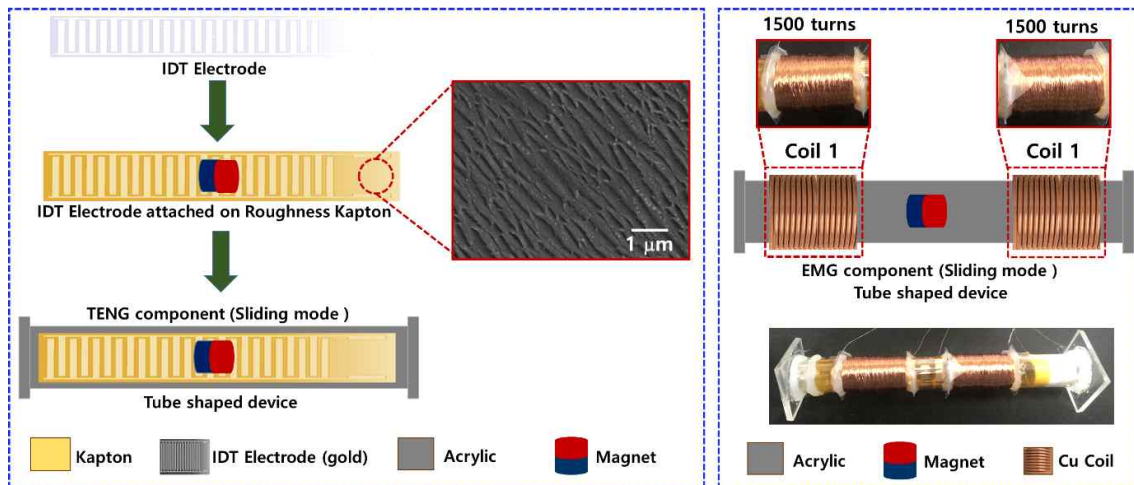


Figure 3.1.1 Schematic diagram of the TENG component with different layers present in the device and the inset shows an FE-SEM image showing the surface roughness made using the Kapton film. The right hand side image shows the EMG components with coils attached and its layers

3.2 Working mechanism

The working mechanism of TENG and EMG component in the SB-HG device is shown in Figure 3.2.1. The TENG component works on contact electrification and electrostatic induction principle between the two triboelectric layers. When the magnet moves on the Kapton layer, the negative charge on the Kapton layer tends to develop a potential difference between the two electrodes of the TENG component leading to drive electrons to flow from one electrode to other with the presence of external load resistance. When the tube moves to opposite direction, the magnet reverses, and the electrons flow back leads to the generation of alternating current.

The mechanism is schematically shown in Figure 3.2.1 with the initial state, sliding and reverse with the electron flow directions. The developed voltage and current were measured in the laboratory using an electrometer, and the developed electrical signals can be stated as follows using the equation.

$$V_{TENG} = \frac{\sigma S}{C} \quad \text{---- (1)}$$

$$I_{TENG} = S \frac{dQ_{SC}}{dt} \quad \text{---- (2)}$$

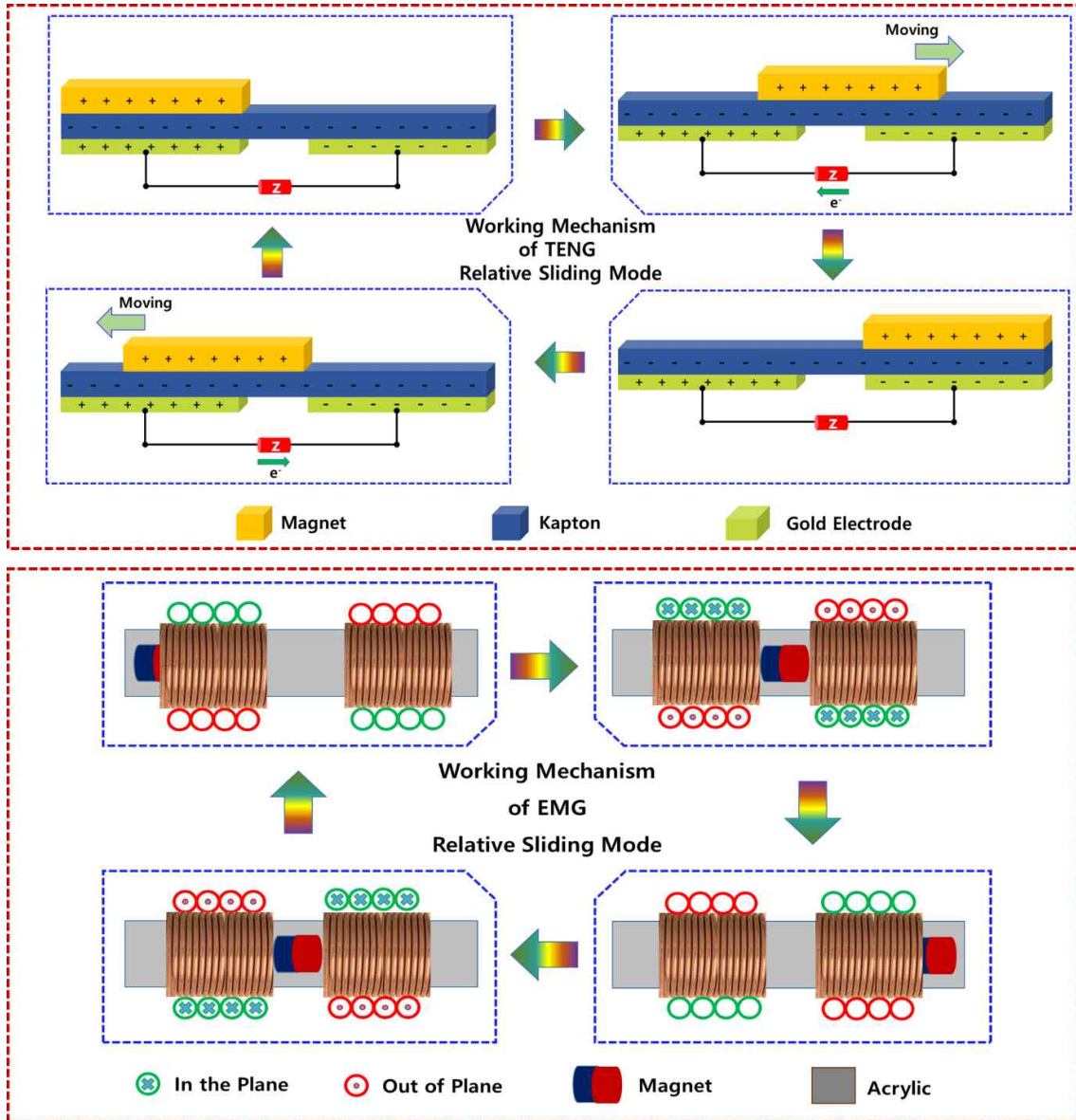


Figure 3.2.1 Working mechanism of TENG and EMG components of the blue energy harvesting hybrid device. The TENG component works on linear sliding mode with the magnet slides over the Kapton film generating electrical output and with the similar motion the magnet moves over the coil wound on the outer side of the PET tube leading to the generation of electric flux in EMG component

Where S is the contact area of the device, C is the capacitance between the electrodes and s is the surface charge density.

With the same mechanical motion the neodymium magnet placed inside the cylindrical tube moves in the inner part of the tube wound with coils, resulting in the development of magnetic flux in the coil as shown in Figure 3.2.1. The magnetic field then makes the electrons to move through the coil. As determined by Lenz's law the direction of movement of electric charge through the coil is responsible for change in flux to utilize a mechanical force contrasting the motion. The generated electrical output of the EMG component could be calculated using the Faraday's law of electromagnetic induction using the below equation

$$V_{EMG} = -N \frac{d\Phi_B}{dt} \text{ ----- (1)}$$

$$I_{EMG} = \frac{V_{OC}}{R} \text{ ----- (2)}$$

Where N is the number of turns, the magnetic flux in each coil and B is the magnetic field.

3.3 Results and discussions

Figure 3.3.1 (a) and (b) shows the triboelectric output with voltage and current with the maximum electrical output of open-circuit voltage of 25 V and short circuit current of 100 nA peak to peak. Similarly, the working mechanism of EMG was shown in Figure 3.2.1 (i to iv). When a linear vibration is applied to the device, the magnet inside the cylinder moves across the coil leads to the production of magnetic flux around the coil which pushes electrons in the copper

wire. The electrons mobility is directly responsible for the electric charge flow which was determined through Lenz's law. The generated output voltage and current from the EMG component can be calculated using Faraday's law. Figure 3.3.1 (c) and (d) shows the electrical output of the EMG with the maximum peak to peak voltage 3 V and a current of 12 mA at an operating frequency of 2 Hz. On the other hand Figure 3.3.2 shows the electrical output of the EMG with 2 coils and the maximum peak to peak voltage 7 V under series connection and a maximum peak to peak output current of 20 mA at an operating frequency of 2 Hz. The current recorded for 2 coils were under parallel connection.

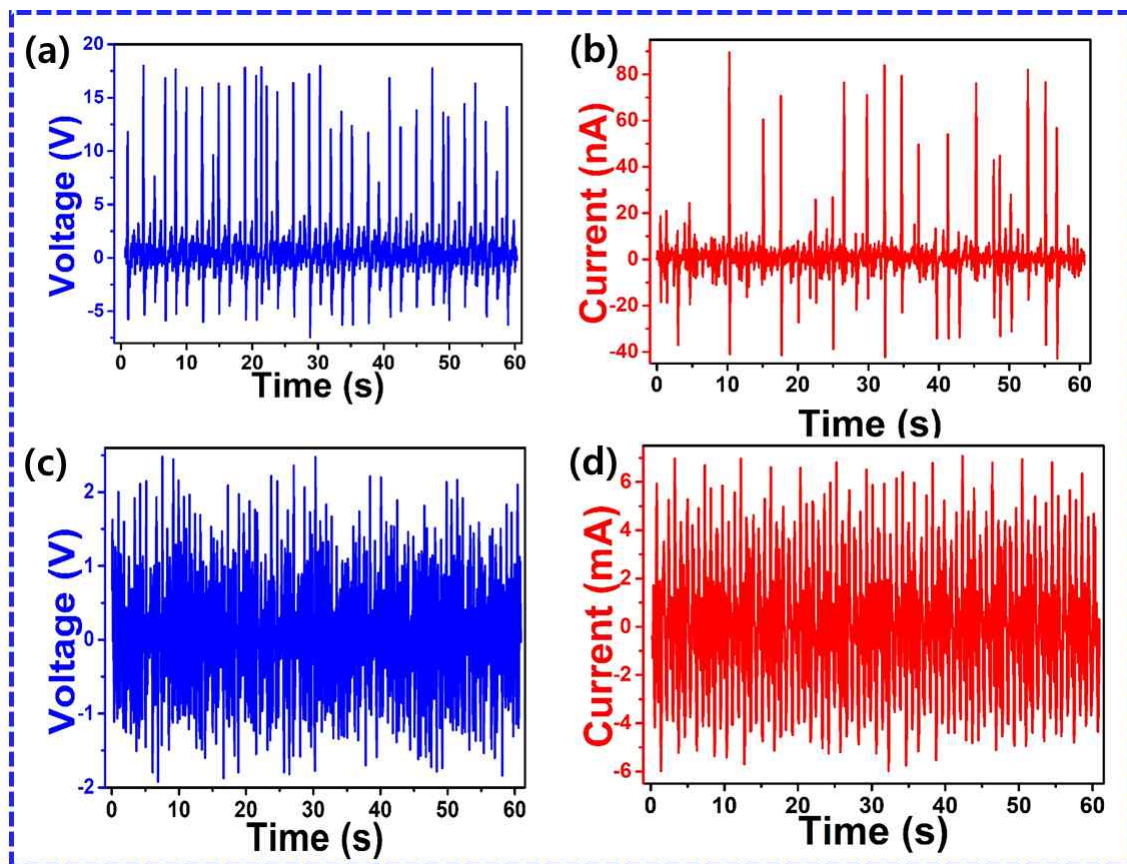


Figure 3.3.1 (a) and (b) voltage and current output of TENG component (c) and (d) voltage and current output of EMG component

Figure 3.3.2 shows the electrical output of the hybrid device with each components separately and also under hybrid configuration with combination of different energy harvesting components. The EMG device shows a rectified electrical output of 2 V and the TENG component shows a rectified electrical output of 6 V. TENG device with 1 EMG coil is then connected in series and the output generated is 7 V and similarly TENG device is the connected with 2 EMG coils.

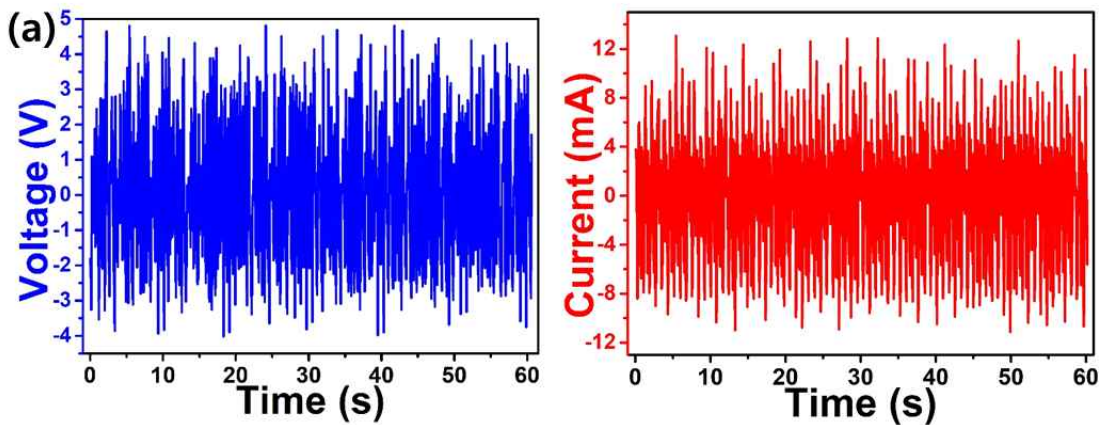


Figure 3.3.2 (a) and (b) voltage and current response of EMG output with both coils connected in series connection for voltage and parallel connection for current measurements

This combination of energy harvesters are leading to the generation of higher output of 8 V under series connection as shown in Figure 3.3.3 (a). Similarly, the current output of the tubular device was measured under parallel connection leading to the generation of higher electrical output due to the connection of components under parallel electrical connections. The measurements were carried out with the acceleration frequency of 2 Hz using a linear motor as shown in Figure 3.3.3 (b). The stability test of the TENG component is shown in Figure 3.3.3 (c) in which the output is stable for a period of 2000 s, which is approximately 33 minutes. The response shows a stable electrical output behavior

without much variation in the electrical output generated. The inset in the stability shows the peak pattern after 1800 s showing there is no decrement in the electrical output of the device, proving that the TENG device can be a stable and reliable energy harvester. The device has been used rigorously in the sliding motion for electrical analysis showing that the device can operate for a long period of time and can be highly suitable for using as a portable power source.

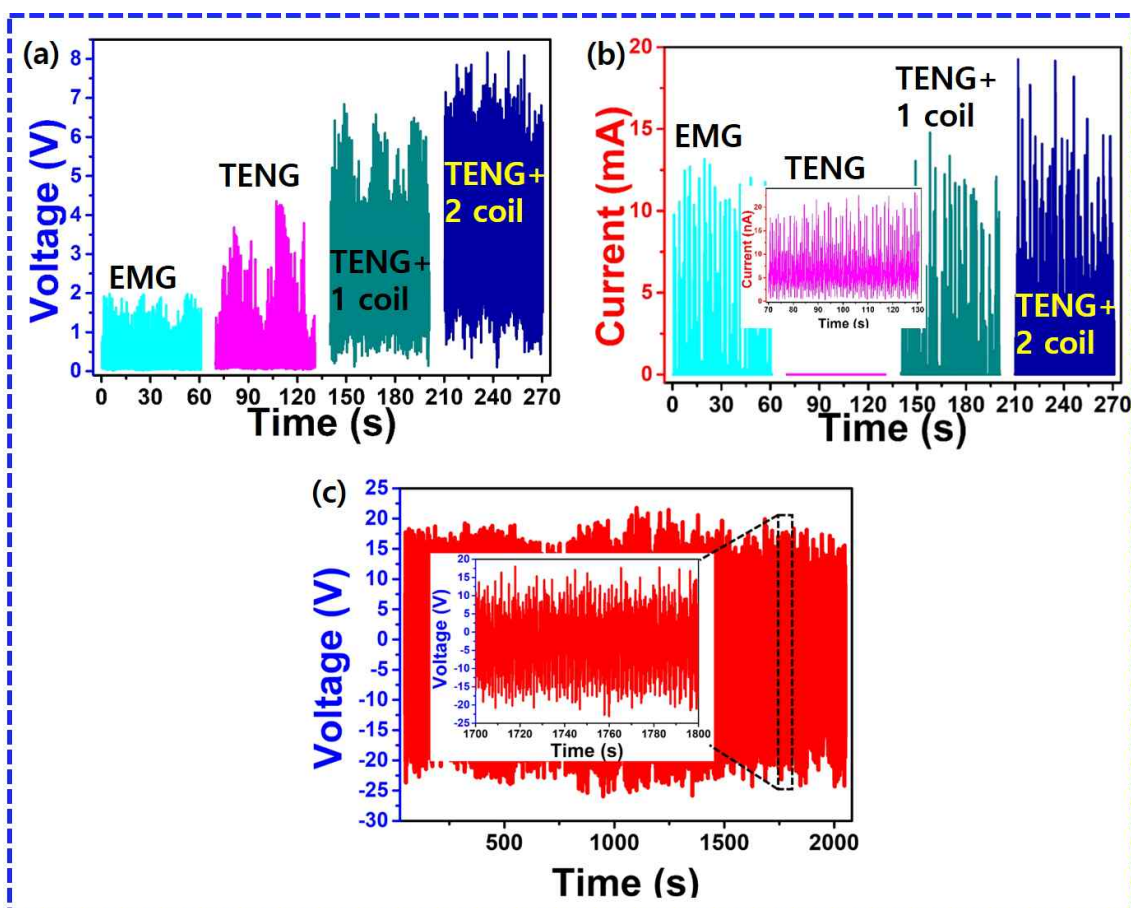


Figure 3.3.3 (a) and (b) voltage and current response of TENG, EMG, TENG + 1 EMG and TENG + 2 EMG compositions (c) stability test of TENG for a period of 2000s using linear motor

The TENG and EMG components are analyzed for different accelerations ranging from 1 m/s², 3 m/s², 5 m/s² and 7 m/s². This analysis shows that the output generation of the energy harvesting component under various accelerations, relating to the output generating capability of the device under various sea circumstances as shown in Figure 3.3.4.

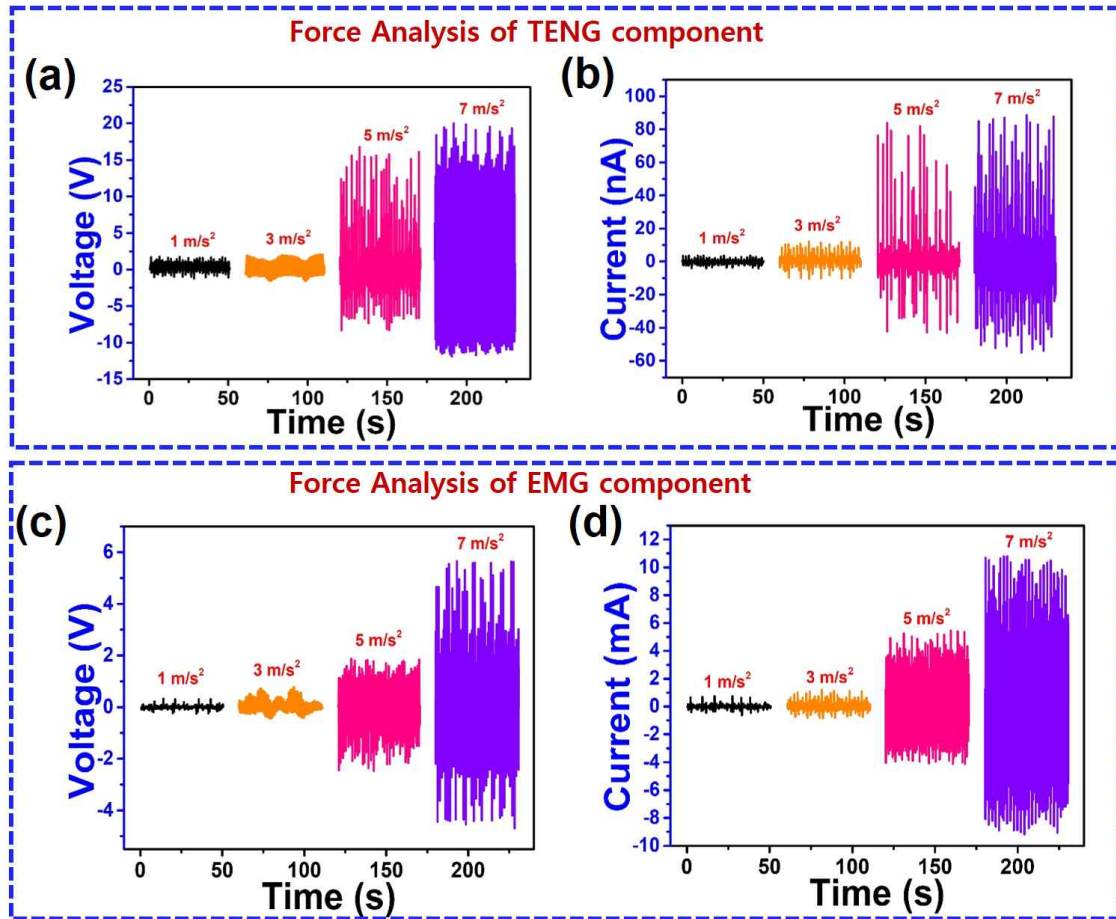


Figure 3.3.4 (a) and (b) force analysis of TENG component (c) and (d) force analysis of EMG component

The real-time energy harvesting capability of the device has been discussed so far and the utilization of the device for powering up electronic devices will be discussed from here. Figure 3.3.5 shows the utilization of hybrid generator for real-time powering of electronic components. Figure 3.3.5 (a) shows the circuit

diagram with rectifiers used for charging the commercial capacitor and also to glow different LEDs. Figure 3.3.5 (b) shows the powering up capacity of hybrid device with high power white, green and red LEDs with the circuit and a capacitor. Figure 3.3.5 also shows the powering up of 80 green LEDs under high power using the device under hybrid combinations. This demonstration proves that the hybrid device is an excellent power source for powering up low power electronic devices and can have the potential to replace batteries in the near future.

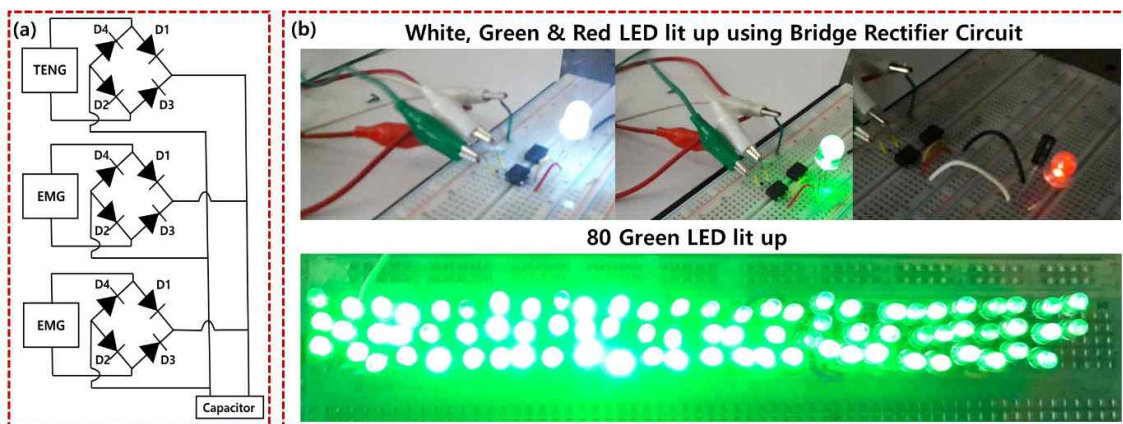


Figure 3.3.5 (a) circuit diagram of capacitor charging and LED lit up (b) high power white, green and red LED lit up using the bridge rectifier circuit and a set of 80 low power green LEDs glowing using hybrid connections

In the similar fashion commercial low power electronic devices such as calculator and hygrometer were powered by using a commercial capacitor with its charging and discharging process. The capacitor charging was made by the hybrid device and during the discharge; the electronic components were powered as shown in Figure 3.3.6 (a) and (b).

To be a stable candidate for powering up electronic devices and components a power management unit is highly desirable. The power management unit regulates the electrical output and gives a stable output of continuous supply

leading to the working of device stable for a longer period. The circuit diagram of PMU and the digital photographic image is shown in Figure 3.3.7 (a) and (b).



Figure 3.3.6 (a) powering up a commercial calculator using the hybrid device with charging a commercial capacitor (b) powering up of a commercial hygrometer for a period of 30 seconds by charging a commercial capacitor

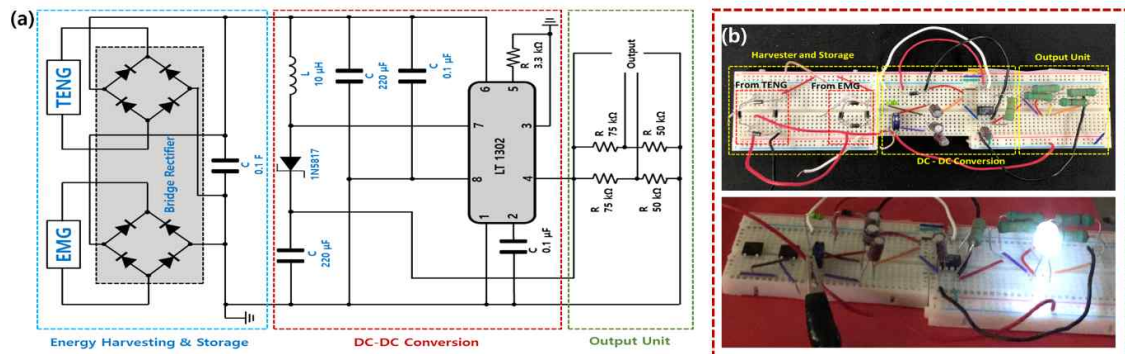


Figure 3.3.7 Power management circuit for the real-time application and (b) shows the real-time image of the developed power management unit and the demonstration of lighting up an white LED using the circuit

The real-time analysis of oil spill detection in ocean was performed in laboratory scale using the hybrid generator device. Figure 3.3.8 (a) shows the schematic of oil spill detection with and without oil and the buoy with the conductors place and connected with PMU and LEDs. Figure 3.3.8 (b) shows the formation of two distinct layers of water and oil in a beaker showing the oil spill formation which can be detected using a hybrid generator buoy device.

Similarly, figure 3.3.8 (c) shows the laboratory test condition of hybrid device for oil spill detection and water wave energy harvesting. Figure 3.3.8 (d) shows the oil spill detection with respect to change in conductivity of the solution with the LED glowing. The trial was made by selecting water samples such as 1 M NaCl solution, sea water, tap water, DI water, oil, oil in sea water and oil in NaCl.

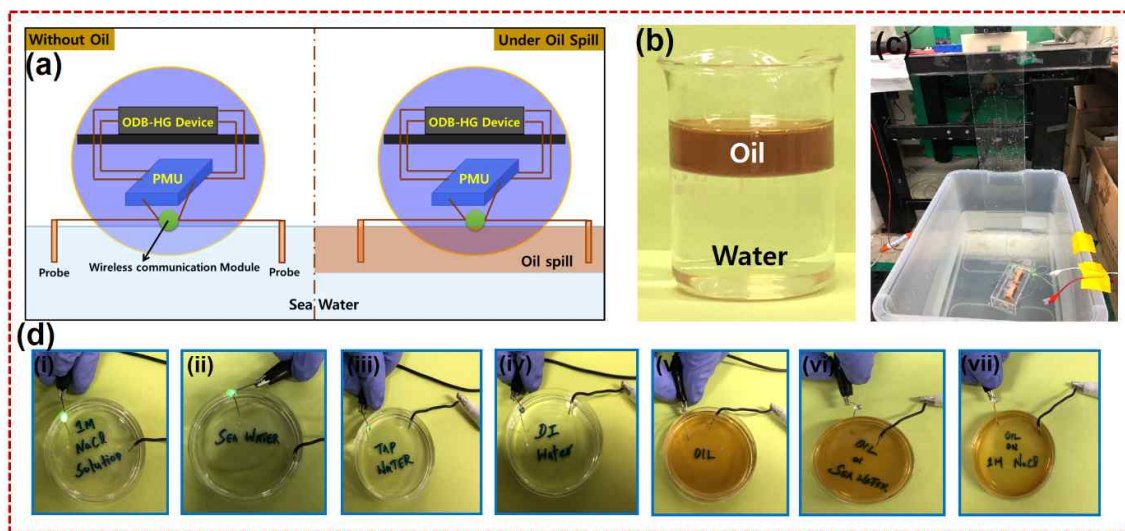


Figure 3.3.8 (a) schematic of the oil spill detection system using the hybrid generator with and without oil (b) two distinct layers of oil and water showing that the oil spill will be on the top of the water due to the high viscosity (c) real time demonstration of oil-spill detection in lab conditions (d) (i-vii) oil spill detection with respect to change in conductivity of the solution with the LED glowing. The trial was made by selecting water samples such as 1 M NaCl solution, sea water, tap water, DI water, oil, oil in sea water and oil in NaCl

Figure 3.3.9 and 3.3.10 shows the oil spill detection under wireless modes using Bluetooth device. The Bluetooth is connected to a mobile phone and the change in conductivity of the ocean is monitored directly under remote mode using Bluetooth module. The change in conductivity triggers an LED and a message in Bluetooth can inform the people remotely.

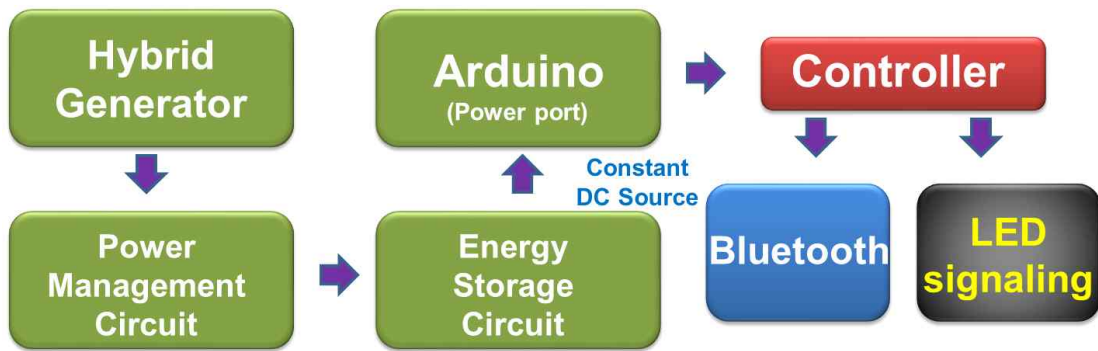


Figure 3.3.9 Schematic of wireless oil spill identification using Bluetooth interface with mobile phone



Figure 3.3.10 (a) blue energy device made with buoy shape which can float in water had setup with the Arduino board and Bluetooth device. The change in conductivity will be informed by Bluetooth messaging and an LED lit up in the buoy

The Table 3.3.1 shows the conductivity value of various solutions used for testing as well as the application of oil spill detection test using the hybrid nanogenerator device.

S. No	solution	conductivity
1	Pure Water	0.05 $\mu\text{s} / \text{cm}$
2	Power Plant Boiler Water	0.05 ~ 1 $\mu\text{s} / \text{cm}$
3	Distilled Water	0.5 $\mu\text{s} / \text{cm}$
4	De-ionized Water	0.1 ~ 10 $\mu\text{s} / \text{cm}$
5	De-Mineralized Water	1 ~ 80 $\mu\text{s} / \text{cm}$
6	Mountain Water	10 $\mu\text{s} / \text{cm}$
7	Drinking Water	0.5 ~ 1 $\mu\text{s} / \text{cm}$
8	Waste-Water	0.9 ~ 9 $\mu\text{s} / \text{cm}$
9	Potable Water Maximum	1.5 $\mu\text{s} / \text{cm}$
10	Brackish Water	1 ~ 80 $\mu\text{s} / \text{cm}$
11	Industrial Process Water	7 ~ 140 $\mu\text{s} / \text{cm}$
12	Ocean Water	53 $\mu\text{s} / \text{cm}$

Table 3.3.1 Conductivity of various water samples

3.4 Conclusion

In conclusion, a tubular shaped single unit hybrid generator composed of TENG and 2 EMG components via a cost-effective has been fabricated for scavenging water wave energy and also used as a self-powered oil spill detection. The device shows its performance in working actively upon various accelerations from 1 m/s^2 to 7 m/s^2 and generates electrical output simultaneously from all the in built energy harvesters such as TENG and 2 EMG units working upon the same motion. The working mechanism of the individual components have been discussed, and the electrical analysis had performed extensively under various accelerations, load matching analysis, capacitor charging, and LED litup. The device generates a maximum electrical output of 25 V and 100 nA current at an acceleration of 5 m/s^2 with an instantaneous power of 200 mW for the TENG component. Similarly, the EMG component generates a maximum output with the voltage of 7 V and a current of 1276 mA at 5 m/s^2 with an instantaneous power 0.7 mW for EMG.

CHAPTER 4

Development of Wind Energy harvesting hybrid generator made of Triboelectric and Electromagnetic components for wind speed and Wind direction monitoring

Highlights

- Herein, we have reported a flutter based hybrid generator (F-HNG) composed of triboelectric nanogenerator (TENG) and electromagnetic generator (EMG) components.
- The triboelectric component is composed of a contact and separation mode using a roughness created fluorinated ethylene polymer (FEP) as a negative material and aluminum as a positive triboelectric material.
- Similarly, the EMG component is made of coil wounded in a horizontal way and attached on the other side of FEP.
- Both the components were housed inside a small rectangular wind tunnel structure. A neodymium magnet is placed on the acrylic on the top side of the structure.
- The contact and separation and electromagnetic actuation work simultaneously upon the same wind force and actuation leads to the generation of electrical output from both the TENG and EMG components independently.
- The TENG component generates a maximum voltage and current of 100 V and 2 mA. Similarly, the EMG component generates a maximum voltage of 200 mV and 200 mA.
- The generated energy can be utilized by lighting up low power electronic

devices and can also be used for charging commercial capacitors.

- The device is then utilized for wind speed monitoring and wind direction monitoring applications

4.1 Experimental Section

4.1.1 Device fabrication and measurements

The device fabrication is composed of an acrylic casing which houses the TENG and EMG components are assembled in a way that they can actuate simultaneously upon impact by wind. The TENG component is made of a contact separation way using Aluminum and FEP, whereas the EMG component works with the front and back motion of coil towards magnet upon wind direction as shown in Figure 4.1.1.

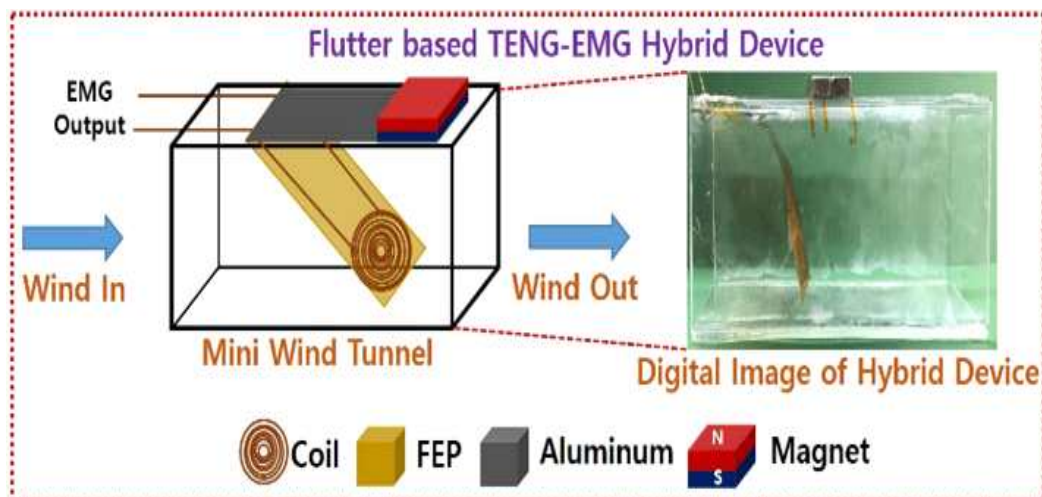


Figure 4.1.1 Schematic of Flutter based hybrid device for scavenging wind energy with TENG and EMG components working simultaneously

Figure 4.1.2 shows various active layers used for the fabrication of wind energy harvesting hybrid generator device. The digital photographic image shows the coil wound on the back side of Kapton layer and the Kapton layer coated with gold as electrode and the Al foil used. The friction between the Kapton and Al creates triboelectric potential and between the coil and magnet activates the EMG components.

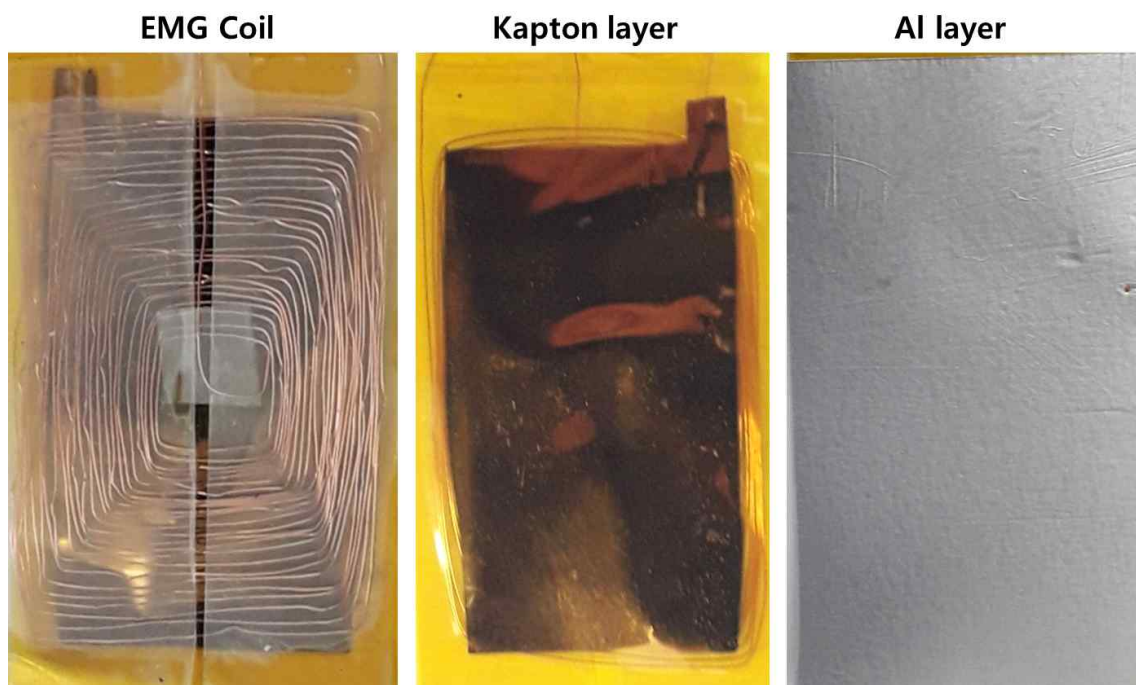


Figure 4.1.2 Various active layers of the wind energy harvesting hybrid generator device with EMG coil, Kapton Layer and Aluminum layer. The friction between Aluminum and Kapton works as TENG component and the EMG coil with magnet generates the EMG component

4.2 Results and discussions

The surface modification in one of the triboelectric layers developed a micro-roughness on the surface of the layer. Here we have developed surface roughness in kapton layer using reactive ion etching technique. Figure 4.2.1 (a)

to (d) shows the FE-SEM morphology of the Kapton film made using the reactive ion etching technique under different conditions as shown in Table 4.1. The conditions are tabulated in Table 4.1 and the corresponding voltage response is shown in Figure 4.2.1 (e).

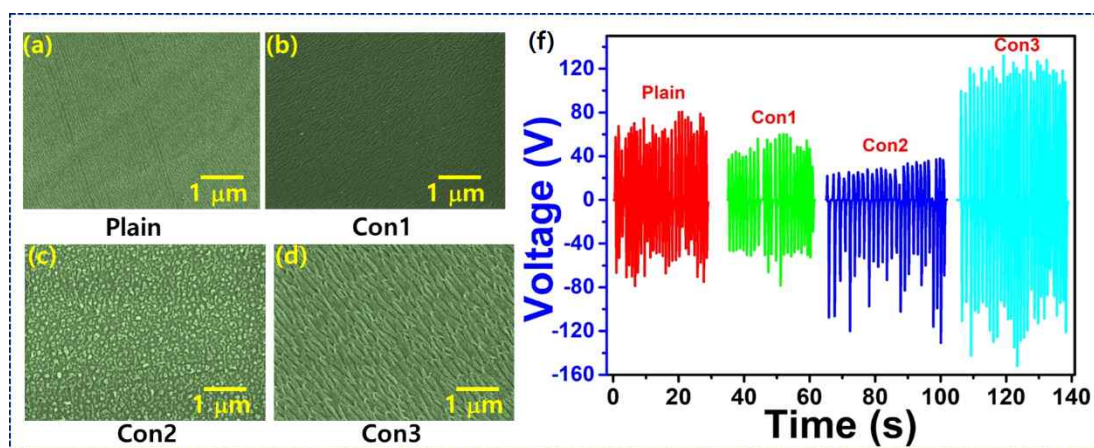


Figure 4.2.1 (a-d) surface morphology of the Kapton film made with the plasma etching process. The surface shows various roughness according to the etching conditions (e) voltage response of Kapton film made with different surface roughness

Power	Condition	O ₂	Ar	CF ₄
220 W	Con1	60	0	0
	Con2	60	20	10
	Con3	60	20	0

Table 4.1 Showing the conditions with respect to gas level (in sccm)

The process of plasma etching is to create micro roughness on the surface of the triboelectric layers. The surface roughness increases the number of contact points which enhances the generation of electrical output upon applying the friction between the triboelectric layers. In plain layer, the number of contact point is one, which makes the output to be less. When the contact point multiplies with the increase in roughness, leads to the generation of higher electrical output.

This mechanism involves interaction between the surface-modified FEP film and the Al electrode with a combination of the triboelectric effect and electrostatic induction. Initially, the top Al electrode layer is in contact with the FEP layer. Next, because of the mechanical motion through wind force, the top layer separates from the FEP layer, and a charge difference occurs across the electrodes. This process induces a flow of electrons from the top electrode to the bottom electrode through an externally connected circuit, as shown in until an equilibrium state is reached This action contributes to the first half-cycle of the alternating current (AC) signal; The second half-cycle is achieved when the top electrode layer approaches the FEP film, inducing a flow of electrons in the opposite direction. The device is then placed in a linear motor and the electrical output of both TENG and EMG were measured. The TENG device generates a maximum voltage and current of 100 V and 2 μ A as shown in Figure 4.2.2. Similarly, the EMG component generates a maximum voltage of 200 mV and 200 mA. This shows that the flutter based device is capable of generating electricity from wind energy as shown in Figure 4.2.3.

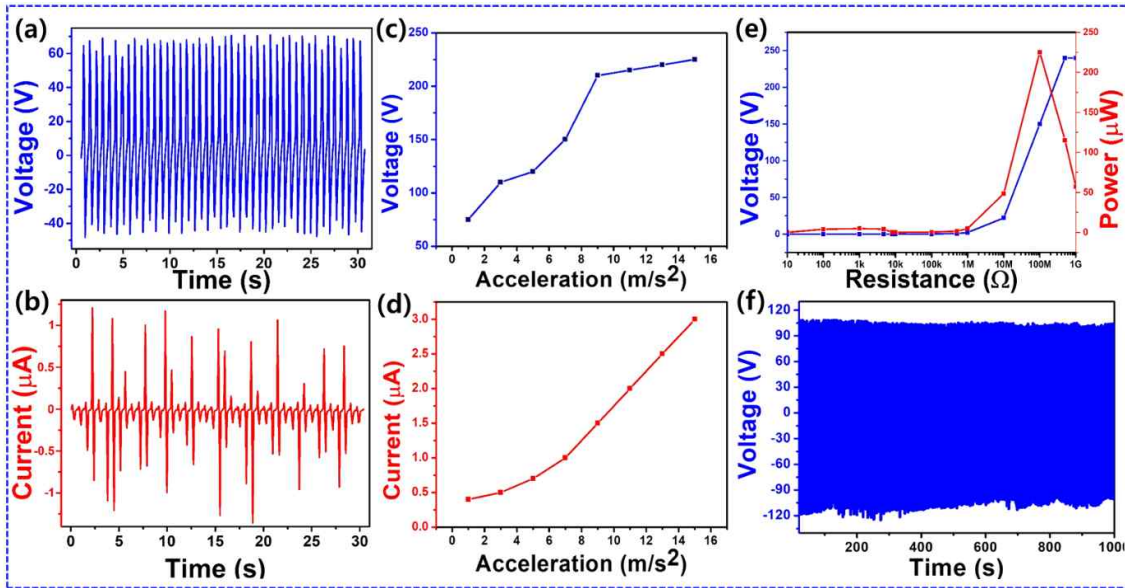


Figure 4.2.2 Electrical output response of the TENG component (a and b) voltage and current output response of the TENG component (c and d) voltage and current of TENG component under different acceleration (e) lead resistance analysis of TENG component with its instantaneous peak power of 225 μW under the resistance of 100 $\text{M}\Omega$ and (f) stability test of TENG for a period of 1000 s at 12 m/s^2 acceleration

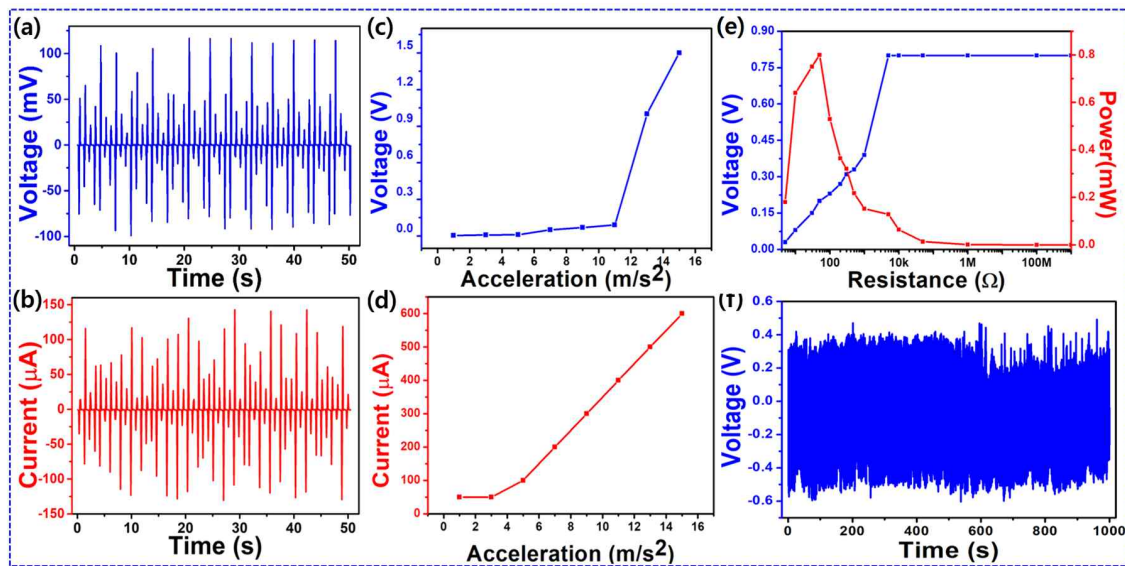


Figure 4.2.3 Electrical output response of the EMG component (a and b) voltage and current output response of the TENG component (c and d) voltage and current of EMG component under different acceleration (e) lead resistance analysis of EMG component with its instantaneous peak power of 0.8 mW under the resistance of 100 Ω and (f) stability test of EMG for a period of 1000 s at 12 m/s^2 acceleration

Further, the device is used for analyzing the instantaneous power density, switching polarity test for the confirmation of electrical output, demonstration of lighting up low power electronics such as glowing LEDs, charging commercial capacitors as shown in Figure 4.2.4. Then the device output under various accelerating frequencies, which can be used for analyzing the energy harvesting capability under various wind speeds. Finally, four devices were used in the top of the building connected in parallel to harvest wind energy and been successfully utilized with the help of an electronic power management circuit.

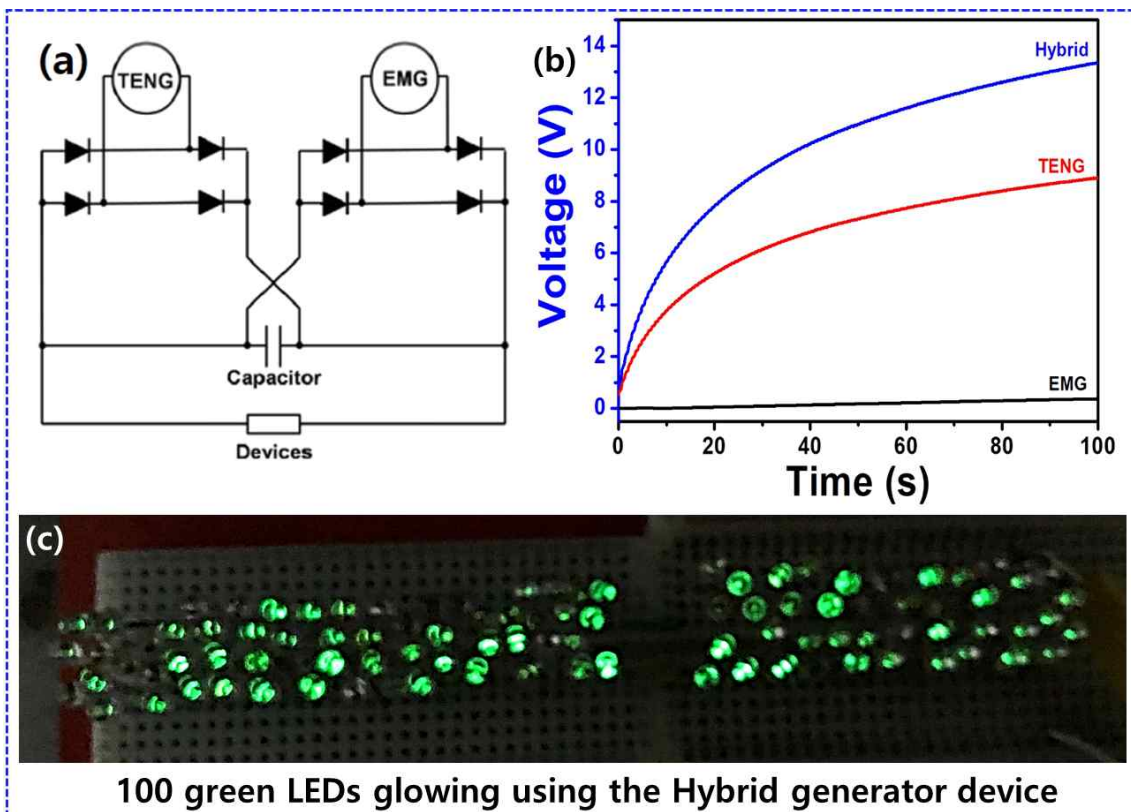


Figure 4.2.4 (a) circuit diagram for charging capacitor and LED lit up connected with TENG and EMG components (b) Capacitor charging using TENG, EMG and Hybrid connections (c) glowing 100 green LEDs using hybrid combination of the flutter based device

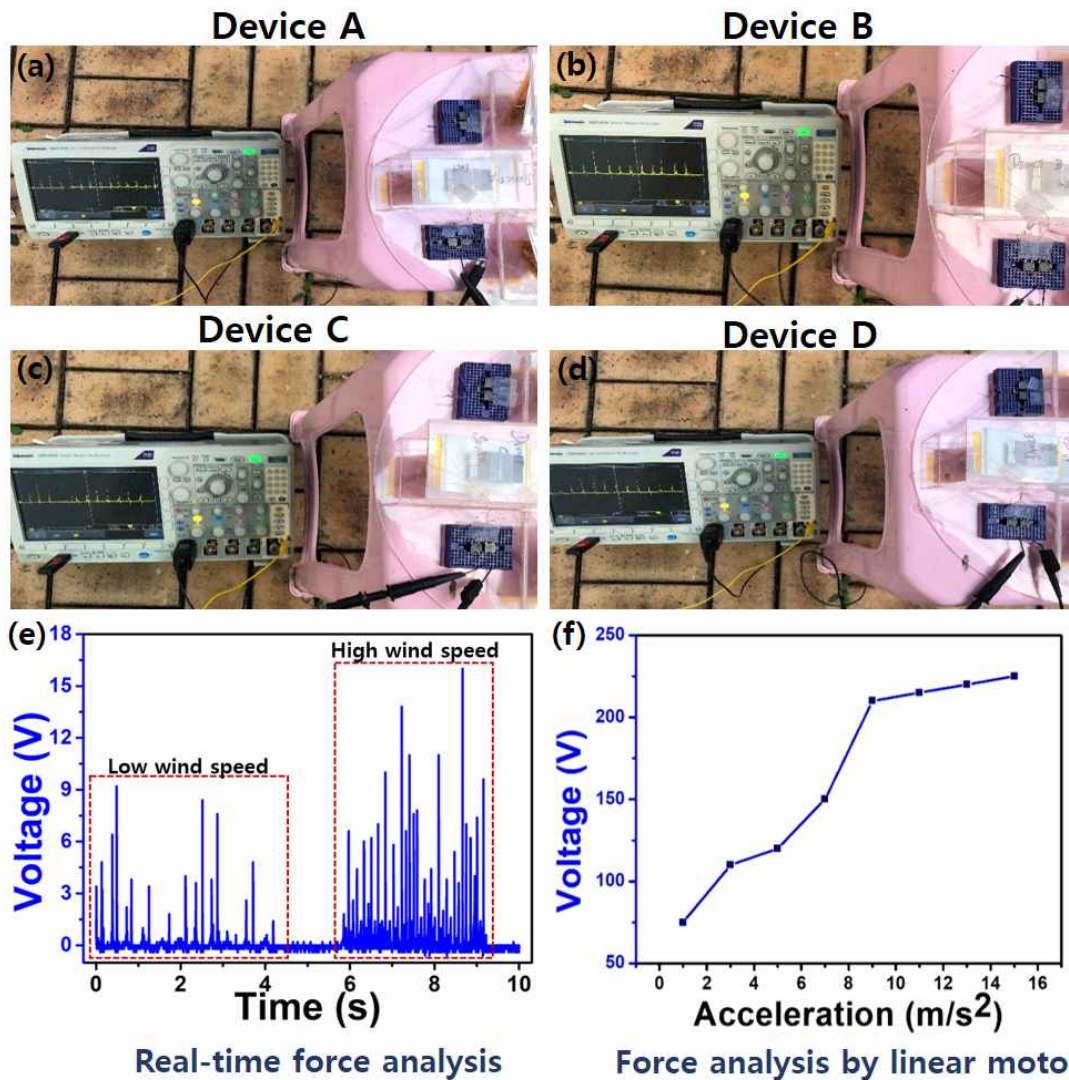


Figure 4.2.5 (a to d) real-time output analysis of the flutter based hybrid device with 4 devices positioned at various directions to monitor the wind direction (e) real-time speed monitoring under low and high speed in comparison with (f) which is measured using linear motor under different accelerations

The device is then used for real-time application of wind speed sensor and wind direction monitoring. Figure 4.2.5 shows the real-time application of flutter based device for wind monitoring and direction monitoring. Figure 4.2.5 (a) to (d) shows the wind direction monitoring with 4 units and the direction could be found out via the output response from the device side. The wind speed is then measured using an oscilloscope and the voltage response level with respect to

the speed indicates the wind speed monitoring using the flutter based device as shown in Figure 4.2.5 (e) and the corresponding electrical output using linear motor is shown in Figure 4.2.5 (f).

4.3 Conclusion

In summary, a flutter based wind energy harvesting device was made using TENG and EMG components housed inside a small wind tunnel which can harvest energy upon simultaneous wind motion and generates electricity independently. The triboelectric component is composed of a contact and separation mode using a roughness created fluorinated ethylene polymer (FEP) as a negative material and aluminum as a positive triboelectric material. Similarly, the EMG component is made of coil wound in a horizontal way and attached on the other side of FEP. The TENG component generates a maximum voltage and current of 100 V and 2 μ A. Similarly, the EMG component generates a maximum voltage of 200 mV and 200 mA. The device is then used to study and analyze its maximum area power density, force analysis and operating commercial electronic devices. Finally, four devices were used in the top of the building connected in parallel to harvest wind energy and been successfully utilized with the help of an electronic power management circuit.

References

1. Nalbant, S. S.; Steacy, S.; Sieh, K.; Natawidjaja, D.; McCloskey, J., Earthquake risk on the Sunda trench. *Nature* **2005**, *435* (7043), 756-757.
2. West, M.; Sánchez, J. J.; McNutt, S. R., Periodically Triggered Seismicity at Mount Wrangell, Alaska, After the Sumatra Earthquake. *Science* **2005**, *308* (5725), 1144-1146.
3. Wang, Z. L.; Song, J., Piezoelectric Nanogenerators Based on Zinc Oxide Nanowire Arrays. *Science* **2006**, *312* (5771), 242-246.
4. Fan, F.-R.; Lin, L.; Zhu, G.; Wu, W.; Zhang, R.; Wang, Z. L., Transparent Triboelectric Nanogenerators and Self-Powered Pressure Sensors Based on Micropatterned Plastic Films. *Nano Letters* **2012**, *12* (6), 3109-3114.
5. Tang, Q.; Yeh, M.-H.; Liu, G.; Li, S.; Chen, J.; Bai, Y.; Feng, L.; Lai, M.; Ho, K.-C.; Guo, H.; Hu, C., Whirligig-inspired triboelectric nanogenerator with ultrahigh specific output as reliable portable instant power supply for personal health monitoring devices. *Nano Energy* **2018**, *47*, 74-80.
6. Pu, X.; Guo, H.; Chen, J.; Wang, X.; Xi, Y.; Hu, C.; Wang, Z. L., Eye motion triggered self-powered mechnosensational communication system using triboelectric nanogenerator. *Science Advances* **2017**, *3* (7).
7. Rasel, M. S.; Maharjan, P.; Salauddin, M.; Rahman, M. T.; Cho, H. O.; Kim, J. W.; Park, J. Y., An impedance tunable and highly efficient triboelectric nanogenerator for large-scale, ultra-sensitive pressure sensing applications. *Nano Energy* **2018**, *49*, 603-613.

8. Liu, Z.; Ma, Y.; Ouyang, H.; Shi, B.; Li, N.; Jiang, D.; Xie, F.; Qu, D.; Zou, Y.; Huang, Y.; Li, H.; Zhao, C.; Tan, P.; Yu, M.; Fan, Y.; Zhang, H.; Wang, Z. L.; Li, Z., Transcatheter Self-Powered Ultrasensitive Endocardial Pressure Sensor. *Advanced Functional Materials* **2019**, *29* (3), 1807560.
9. Fan, X.; Chen, J.; Yang, J.; Bai, P.; Li, Z.; Wang, Z. L., Ultrathin, Rollable, Paper-Based Triboelectric Nanogenerator for Acoustic Energy Harvesting and Self-Powered Sound Recording. *ACS Nano* **2015**, *9* (4), 4236-4243.
10. Yang, Y.; Zhang, H.; Lin, Z.-H.; Zhou, Y. S.; Jing, Q.; Su, Y.; Yang, J.; Chen, J.; Hu, C.; Wang, Z. L., Human Skin Based Triboelectric Nanogenerators for Harvesting Biomechanical Energy and as Self-Powered Active Tactile Sensor System. *ACS Nano* **2013**, *7* (10), 9213-9222.
11. Guo, H.; Chen, J.; Tian, L.; Leng, Q.; Xi, Y.; Hu, C., Airflow-Induced Triboelectric Nanogenerator as a Self-Powered Sensor for Detecting Humidity and Airflow Rate. *ACS Applied Materials & Interfaces* **2014**, *6* (19), 17184-17189.
12. Chen, J.; Zhu, G.; Yang, W.; Jing, Q.; Bai, P.; Yang, Y.; Hou, T.-C.; Wang, Z. L., Harmonic-Resonator-Based Triboelectric Nanogenerator as a Sustainable Power Source and a Self-Powered Active Vibration Sensor. *Advanced Materials* **2013**, *25* (42), 6094-6099.
13. Wang, X.; Peng, D.; Huang, B.; Pan, C.; Wang, Z. L., Piezophotonic effect based on mechanoluminescent materials for advanced flexible optoelectronic applications. *Nano Energy* **2019**, *55*, 389-400.

14. Purusothaman, Y.; Alluri, N. R.; Chandrasekhar, A.; Vivekananthan, V.; Kim, S. J., Regulation of Charge Carrier Dynamics in ZnO Microarchitecture-Based UV/Visible Photodetector via Photonic-Strain Induced Effects. *Small* **2018**, *14* (11), 1703044.
15. Yang, X.; Hu, G.; Gao, G.; Chen, X.; Sun, J.; Wan, B.; Zhang, Q.; Qin, S.; Zhang, W.; Pan, C.; Sun, Q.; Wang, Z. L., Coupled Ion-Gel Channel-Width Gating and Piezotronic Interface Gating in ZnO Nanowire Devices. *Advanced Functional Materials* *0* (0), 1807837.
16. Zhao, C.; Feng, H.; Zhang, L.; Li, Z.; Zou, Y.; Tan, P.; Ouyang, H.; Jiang, D.; Yu, M.; Wang, C.; Li, H.; Xu, L.; Wei, W.; Li, Z., Highly Efficient In Vivo Cancer Therapy by an Implantable Magnet Triboelectric Nanogenerator. *Advanced Functional Materials* *0* (0), 1808640.
17. Selvarajan, S.; Alluri, N. R.; Chandrasekhar, A.; Kim, S.-J., BaTiO₃ nanoparticles as biomaterial film for self-powered glucose sensor application. *Sensors and Actuators B: Chemical* **2016**, *234*, 395-403.
18. Alluri, N. R.; Selvarajan, S.; Chandrasekhar, A.; Balasubramaniam, S.; Jeong, J. H.; Kim, S.-J., Self powered pH sensor using piezoelectric composite worm structures derived by ionotropic gelation approach. *Sensors and Actuators B: Chemical* **2016**, *237*, 534-544.
19. Vivekananthan, V.; Alluri, N. R.; Purusothaman, Y.; Chandrasekhar, A.; Selvarajan, S.; Kim, S.-J., Biocompatible Collagen Nanofibrils: An Approach for Sustainable Energy Harvesting and Battery-Free Humidity Sensor Applications. *ACS Applied Materials & Interfaces* **2018**, *10* (22), 18650-18656.

20. Guan, H.; Zhong, T.; He, H.; Zhao, T.; Xing, L.; Zhang, Y.; Xue, X., A self-powered wearable sweat-evaporation-biosensing analyzer for building sports big data. *Nano Energy* **2019**, *59*, 754-761.
21. Han, W.; He, H.; Zhang, L.; Dong, C.; Zeng, H.; Dai, Y.; Xing, L.; Zhang, Y.; Xue, X., A Self-Powered Wearable Noninvasive Electronic-Skin for Perspiration Analysis Based on Piezo-Biosensing Unit Matrix of Enzyme/ZnO Nanoarrays. *ACS Applied Materials & Interfaces* **2017**, *9* (35), 29526-29537.
22. Pu, X.; Guo, H.; Tang, Q.; Chen, J.; Feng, L.; Liu, G.; Wang, X.; Xi, Y.; Hu, C.; Wang, Z. L., Rotation sensing and gesture control of a robot joint via triboelectric quantization sensor. *Nano Energy* **2018**, *54*, 453-460.
23. Fan, F.-R.; Tian, Z.-Q.; Lin Wang, Z., Flexible triboelectric generator. *Nano Energy* **2012**, *1* (2), 328-334.
24. Yang, H.; Wang, M.; Deng, M.; Guo, H.; Zhang, W.; Yang, H.; Xi, Y.; Li, X.; Hu, C.; Wang, Z., A full-packaged rolling triboelectric-electromagnetic hybrid nanogenerator for energy harvesting and building up self-powered wireless systems. *Nano Energy* **2019**, *56*, 300-306.
25. Seol, M.-L.; Han, J.-W.; Park, S.-J.; Jeon, S.-B.; Choi, Y.-K., Hybrid energy harvester with simultaneous triboelectric and electromagnetic generation from an embedded floating oscillator in a single package. *Nano Energy* **2016**, *23*, 50-59.
26. Zhao, J.; Zhen, G.; Liu, G.; Bu, T.; Liu, W.; Fu, X.; Zhang, P.; Zhang, C.; Wang, Z. L., Remarkable merits of triboelectric nanogenerator than electromagnetic generator for harvesting small-amplitude mechanical energy. *Nano Energy* **2019**, *61*, 111-118.

27. Askari, H.; Asadi, E.; Saadatnia, Z.; Khajepour, A.; Khamesee, M. B.; Zu, J., A flexible tube-based triboelectric–electromagnetic sensor for knee rehabilitation assessment. *Sensors and Actuators A: Physical* **2018**, *279*, 694-704.
28. Guo, Y.; Chen, Y.; Ma, J.; Zhu, H.; Cao, X.; Wang, N.; Wang, Z. L., Harvesting wind energy: A hybridized design of pinwheel by coupling triboelectrification and electromagnetic induction effects. *Nano Energy* **2019**, *60*, 641-648.
29. Askari, H.; Saadatnia, Z.; Asadi, E.; Khajepour, A.; Khamesee, M. B.; Zu, J., A flexible hybridized electromagnetic-triboelectric multi-purpose self-powered sensor. *Nano Energy* **2018**, *45*, 319-329.
30. Saadatnia, Z.; Asadi, E.; Askari, H.; Zu, J.; Esmailzadeh, E., Modeling and performance analysis of duck-shaped triboelectric and electromagnetic generators for water wave energy harvesting. *International Journal of Energy Research* **2017**, *41* (14), 2392-2404.
31. Liu, L.; Tang, W.; Chen, B.; Deng, C.; Zhong, W.; Cao, X.; Wang, Z. L., A Self-Powered Portable Power Bank Based on a Hybridized Nanogenerator. *Advanced Materials Technologies* **2018**, *3* (3), 1700209.
32. Askari, H.; Asadi, E.; Saadatnia, Z.; Khajepour, A.; Khamesee, M. B.; Zu, J., A hybridized electromagnetic-triboelectric self-powered sensor for traffic monitoring: concept, modelling, and optimization. *Nano Energy* **2017**, *32*, 105-116.

33. Wang, W.; Xu, J.; Zheng, H.; Chen, F.; Jenkins, K.; Wu, Y.; Wang, H.; Zhang, W.; Yang, R., A spring-assisted hybrid triboelectric–electromagnetic nanogenerator for harvesting low-frequency vibration energy and creating a self-powered security system. *Nanoscale* **2018**, *10* (30), 14747-14754.
34. Quan, T.; Wu, Y.; Yang, Y., Hybrid electromagnetic–triboelectric nanogenerator for harvesting vibration energy. *Nano Research* **2015**, *8* (10), 3272-3280.
35. Seol, M.-L.; Jeon, S.-B.; Han, J.-W.; Choi, Y.-K., Ferrofluid-based triboelectric-electromagnetic hybrid generator for sensitive and sustainable vibration energy harvesting. *Nano Energy* **2017**, *31*, 233-238.
36. Lu, C. X.; Han, C. B.; Gu, G. Q.; Chen, J.; Yang, Z. W.; Jiang, T.; He, C.; Wang, Z. L., Temperature Effect on Performance of Triboelectric Nanogenerator. *Advanced Engineering Materials* **2017**, *19* (12), 1700275.
37. Kim, D.; Jin, I. K.; Choi, Y.-K., Ferromagnetic nanoparticle-embedded hybrid nanogenerator for harvesting omnidirectional vibration energy. *Nanoscale* **2018**, *10* (26), 12276-12283.

Appendix: Publications

1. Venkateswaran Vivekananthan, **Woo Joong Kim**, Nagamalleswara Rao Alluri, Yuvasree Purusothaman, K. S. Abisegapriyan and Sang-Jae Kim "A sliding mode contact electrification based triboelectric-electromagnetic hybrid generator for small-scale biomechanical energy harvesting" *Micro and Nano Syst Lett*, 2019, 7, 14.
2. Vivekananthan V, Chandrasekhar A, Alluri NR, Purusothaman Y, **Kim WJ**, Kang CN, Kim SJ "A flexible piezoelectric composite nanogenerator based on doping enhanced lead-free nanoparticles" *Materials Letters*. 2019 Aug 15;249:73-6.

Appendix: Conferences

1. **Woo Joong Kim**, Venkateswaran Vivekananthan, Gaurav Khandelwal, Arunkumar Chandrasekar, Sang-Jae Kim “Triboelectric-Electromagnetic Hybrid Generator for Wind Energy Harvesting” ICMR 2019, Nov. 27, 2019.
2. Vivekananthan Venkateswaran, Nagamalleswara Rao Alluri, Yuvasree Purusothaman, Nirmal Prashanth Maria Joseph Raj, **Woo Joong Kim**, Sang-Jae Kim “A Water Resistant Triboelectric Nanogenerator as a Bio-mechanical Energy Harvester and a Self-powered Pressure Sensor” ICMR 2019, Nov. 27, 2019.
3. **Woo Joong kim**, Venkateswaran Vivekananthan, Gaurav Khandelwal, Sang-Jae kim “A Highly Reliable Flutter Driven Triboelectric-electromagnetic Hybrid Generator for Efficient Wind Energy Harvesting” KSME 2019, Nov. 15, 2019
4. Venkateswaran Vivekananthan, Nagamalleswara Rao Alluri, Yuvasree Purusothaman, **Woo Joong kim**, Sang-Jae Kim “A High Output Triboelectric and Piezoelectric Hybrid Nanogenerator Based on $K_{0.5}Na_{0.5}NbO_3$ Nanoparticles into PDMS Composite Films” KSME 2019, Nov. 15, 2019
5. Vivekananthan Venkateswaran, Nagamalleswara Rao Alluri, Yuvasree Purusothaman, **Woo Joong Kim**, Sang-Jae Kim “Fabrication of Self-Powered Sensors using Doped Piezoelectric Nanogenerators” KSDT 2019, May. 9, 2019
6. **Woo Joong Kim**, Venkateswaran Vivekananthan, Gaurav Khandelwal, Arunkumar Chandrasekhar, Sang-Jae Kim “A combined Triboelectric-Electromagnetic cylindrical hybrid nanogenerator for water wave energy scavenging” 21th KMEMS, Apr. 6, 2019

7. Venkateswaran Vivekananthan, Arunkumar Chandrasekhar, Nagamalleswara Rao Alluri, Yuvasree Purusothaman, **Woo Joong Kim**, Sang-Jae Kim “Development of a hybrid energy harvester based on ferromagnetic Fe₂O₃nanoparticles”21thKMEMS, Apr.6,2019
8. **Woo Joong Kim**, Venkateswaran Vivekananthan, Gaurav Khandelwal, Arunkumar Chandrasekhar, Sang-Jae Kim “블루에너지 수확을 위한 원기동형 마찰전기-전자기 하이브리드 발전기의 작동신뢰성” KSME 2019, Feb. 27, 2019
9. **Woo Joong Kim**, Arunkumar Chandrasekhar, Gaurav Khandelwal, Sang-Jae Kim “Tube Shaped Hybridized Triboelectric Nanogenerator for Scavenging Broad-Mechanical Energy” ENGE 2018, Nov. 14, 2018
10. Arunkumar Chandrasekhar, Gaurav Khandelwal, Vivekananthan Venkateswaran, **Woo Joong Kim**, Sang-Jae Kim “Triboelectric Nanogenerator as Smart Gadgets and Its Self-Powered Applications” ENGE 2018, Nov. 14, 2018
11. **Woo Joong Kim**, Arunkumar Chandrasekhar, Gaurav Khandelwal, Sang-Jae Kim “Fabrication of hybrid generator for tracing fishing net buoy” KSPSE 2018, Nov. 1, 2018
12. **Woo Joong Kim**, Arunkumar Chandrasekhar, Sang-Jae Kim “Hybrid Triboelectric nanogenerator as a Smart Buoy for Scavenging Water Wave Energy” KPS 2018, Aug. 6, 2018
13. **Woo Joong Kim**, Arunkumar Chandrasekhar, Oh Gil Seop, Kim Gwan Yong, Kim Tae Beom, Sang-Jae Kim “Blue Energy Scavenging Smart Buoy using Hybrid Triboelectric Nanogenerator” JSST 2017, May. 25, 2017

Appendix: List of awards

1. Vivekananthan Venkateswaran, Nagamalleswara Rao Alluri, Yuvasree Purusothaman, Nirmal Prashanth Maria Joseph Raj, **Woo Joong Kim**, Sang-Jae Kim “A Water Resistant Triboelectric Nanogenerator as a Bio-mechanical Energy Harvester and a Self-powered Pressure Sensor” ICMR 2019, Nov. 27, 2019 – **Best poster award**
2. Vivekananthan Venkateswaran, Nagamalleswara Rao Alluri, Yuvasree Purusothaman, **Woo Joong Kim**, Sang-Jae Kim “Fabrication of Self-Powered Sensors using Doped Piezoelectric Nanogenerators” KSDT 2019, May. 9, 2019 – **Best poster award**

Declaration

I, **Woo Joong Kim**, hereby declare that the thesis entitled “**Development of hybrid generator using triboelectric-electromagnetic components for scavenging wind and water wave energy**”, submitted to the Jeju National University, in partial fulfillment of the requirements for the award of the **Degree of Master of Engineering in Department of Mechatronics Engineering** is a record of original and independent research work done and published by me during the period March 2018 to February 2020 under the supervision and guidance of **Prof. Sang Jae Kim**, Department of Mechatronics Engineering, Jeju National University. This thesis solely based on our publication in reputed journals, and it has not been formed on the basis from the award of any other Degree / Diploma / Associateship / Fellowship.

Woo Joong Kim